Article

Cell Host & Microbe

The natural product chlorotonil A preserves colonization resistance and prevents relapsing *Clostridioides difficile* infection

Graphical abstract

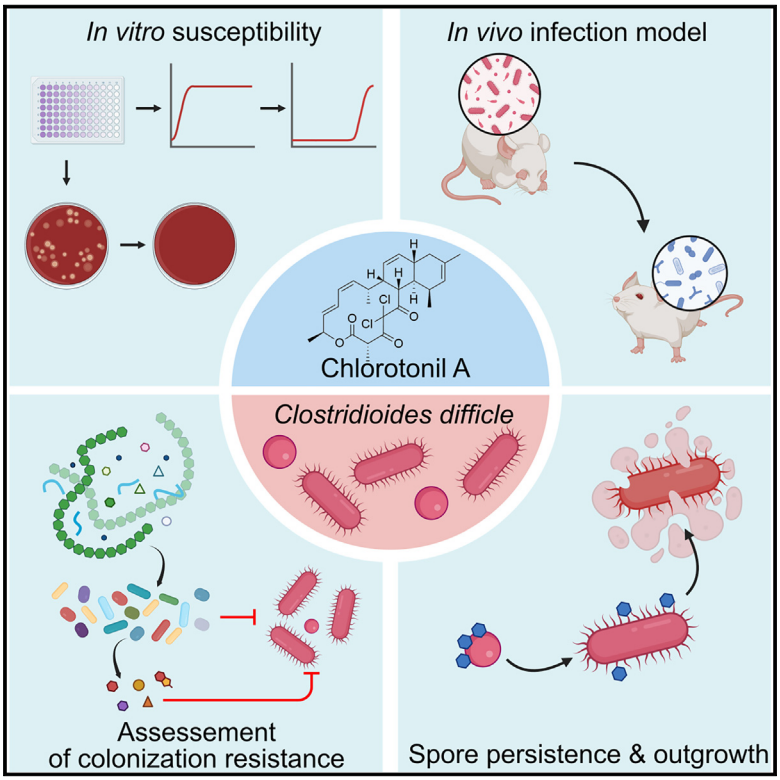

Authors

Arne Bublitz, Madita Brauer, Stefanie Wagner, ..., Rolf Müller, Thilo M. Fuchs, Till Strowig

Correspondence

thilom.fuchs@fli.de (T.M.F.), till.strowig@helmholtz-hzi.de (T.S.)

In brief

Bublitz et al. identified that the natural product chlorotonil A (ChA) has antimicrobial activity against *Clostridioides difficile*, preventing relapsing disease in a mouse model. Favorable properties of ChA synergize for this protective effect, including reduced microbiome damage, preservation of colonization resistance, and prevention of vegetative cell outgrowth from spores.

Highlights

- Chlorotonil A (ChA) has antimicrobial activity against *Clostridioides difficile*
- ChA prevents relapsing *C. difficile* infection in a mouse model
- Unlike vancomycin, ChA preserves colonization resistance against *C. difficile*
- ChA is retained in *C. difficile* spores, preventing outgrowth of vegetative cells

Bublitz et al., 2023, Cell Host & Microbe *31*, 734–750
May 10, 2023
https://doi.org/10.1016/j.chom.2023.04.003

CellPress

CellPress
OPEN ACCESS

Cell Host & Microbe

Article

The natural product chlorotonil A preserves colonization resistance and prevents relapsing *Clostridioides difficile* infection

Arne Bublitz,[1] Madita Brauer,[2,3,16] Stefanie Wagner,[4,16] Walter Hofer,[5,15] Mathias Müsken,[6] Felix Deschner,[5,15] Till R. Lesker,[1] Meina Neumann-Schaal,[7,8] Lena-Sophie Paul,[4] Ulrich Nübel,[8,9,10] Jürgen Bartel,[11] Andreas M. Kany,[5,15] Daniela Zühlke,[2] Steffen Bernecker,[12] Rolf Jansen,[12] Susanne Sievers,[2] Katharina Riedel,[2,3] Jennifer Herrmann,[5,10,15] Rolf Müller,[5,10,15] Thilo M. Fuchs,[4,*] and Till Strowig[1,10,13,14,17,*]

[1]Department of Microbial Immune Regulation, Helmholtz Center for Infection Research, Braunschweig, Germany
[2]Institute of Microbiology, Department of Microbial Physiology and Molecular Biology, University of Greifswald, Greifswald, Germany
[3]Institute of Marine Biotechnology e.V., Greifswald, Germany
[4]Friedrich-Loeffler-Institut, Institute of Molecular Pathogenesis, Jena, Germany
[5]Department of Microbial Natural Products, Helmholtz Institute for Pharmaceutical Research Saarland (HIPS), Helmholtz Centre for Infection Research (HZI), Saarbrücken, Germany
[6]Central Facility for Microscopy, Helmholtz Center for Infection Research (HZI), Braunschweig, Germany
[7]Bacterial Metabolomics, Leibniz Institute DSMZ – German Collection of Microorganisms and Cell Cultures, Braunschweig, Germany
[8]Braunschweig Integrated Center of Systems Biology (BRICS), Technical University, Braunschweig, Germany
[9]Microbial Genome Research, Leibniz Institute DSMZ – German Collection of Microorganisms and Cell Cultures, Braunschweig, Germany
[10]German Center for Infection Research (DZIF), Partner Site Hannover-Braunschweig, Braunschweig, Germany
[11]Institute of Microbiology, Department of Microbial Proteomics, University of Greifswald, Greifswald, Germany
[12]Department of Microbial Drugs, Helmholtz Center for Infection Research (HZI), Braunschweig, Germany
[13]Cluster of Excellence RESIST (EXC 2155), Hannover Medical School, Hannover, Germany
[14]Centre for Individualised Infection Medicine (CiiM), Hannover, Germany
[15]Department of Pharmacy, Saarland University, Saarbrücken, Germany
[16]These authors contributed equally
[17]Lead contact
*Correspondence: thilom.fuchs@fli.de (T.M.F.), till.strowig@helmholtz-hzi.de (T.S.)
https://doi.org/10.1016/j.chom.2023.04.003

SUMMARY

Clostridioides difficile infections (CDIs) remain a healthcare problem due to high rates of relapsing/recurrent CDIs (rCDIs). Breakdown of colonization resistance promoted by broad-spectrum antibiotics and the persistence of spores contribute to rCDI. Here, we demonstrate antimicrobial activity of the natural product class of chlorotonils against *C. difficile*. In contrast to vancomycin, chlorotonil A (ChA) efficiently inhibits disease and prevents rCDI in mice. Notably, ChA affects the murine and porcine microbiota to a lesser extent than vancomycin, largely preserving microbiota composition and minimally impacting the intestinal metabolome. Correspondingly, ChA treatment does not break colonization resistance against *C. difficile* and is linked to faster recovery of the microbiota after CDI. Additionally, ChA accumulates in the spore and inhibits outgrowth of *C. difficile* spores, thus potentially contributing to lower rates of rCDI. We conclude that chlorotonils have unique antimicrobial properties targeting critical steps in the infection cycle of *C. difficile*.

INTRODUCTION

Clostridioides difficile is an anaerobic enteropathogen of both humans and animals. Although asymptomatic carriage with *C. difficile* can be found in the intestinal tract of mammals,[1] *C. difficile* has emerged as the most frequent agent of antibiotic-associated diarrhea, causing mild to severe forms of colitis.[2] Even after an initially successful antibiotic therapy, recurrence rates reach up to 20%, with mortality rates of up to 10%.[3] Despite currently low antibiotic resistance rates of *C. difficile* to the clinically relevant antibiotics metronidazole, vancomycin, and fidaxomicin,[4] therapy of *C. difficile* infections (CDIs) is still challenging. Moreover, the potential emergence and spread of antibiotic-resistant strains of *C. difficile* should preemptively be addressed by the search for new therapeutics against CDI.

A prerequisite for CDI is the breakdown of the colonization resistance (CR) against *C. difficile*, e.g., by antibiotics, in concert with other risk factors such as age and immune deficiencies.[5–7] Conversely, recovery of the intestinal microbial community and concomitantly CR helps to combat CDI and to prevent recurrence from remaining *C. difficile* spores and biofilm-associated cells.[8,9]

Consequently, antibiotics, which cause collateral damage to many members of the microbiota, are linked to high CDI recurrence rates.[10–12] A metabolic property of the microbiota identified to contribute to CR against *C. difficile* is the conversion of conjugated primary bile acids (BAs) to secondary BA through microbial enzymes, although a recent study showed complete protection against CDI in a BA-independent manner.[13–15] Along these lines, sequestration of nutrients preferred by *C. difficile*, such as proline and branched-chain amino acids (AAs), in the so-called Stickland-reactions was identified to significantly contribute to CR.[16,17] Similarly, although *C. difficile* is metabolically highly versatile, there is strong evidence that it is unable to compete with other microbes *in vivo* in the absence of proline fermentation.[16,18–20] In contrast to the protective functions of the microbiota, cross feeding from commensals may also reinforce infection.[17,19]

Since broad-spectrum antibiotics significantly damage the microbiota and thus potentially promote relapsing/recurrent CDI (rCDI), their avoidance in the treatment of certain bacterial infections is justified.[21] Moreover, this consideration has urged the development of narrow-range antibiotics, such as fidaxomicin, with a high antimicrobial activity toward *C. difficile*,[22] although resistance against fidaxomicin has already been observed.[23] CDI treatment is complicated by the ability of *C. difficile* to form dormant spores that are resistant against antibiotics and can only be killed by specific, disinfectant-type chemicals.[24] Signals inducing sporulation are diverse environmental stimuli, such as nutrient starvation and quorum sensing, resulting in a continuous production of spores during CDI.[25] Spores not only contribute to the spread of CDI to other patients but also to rCDI within a patient. Similarly to sporulation, spore germination is a complex process induced when specific germinant receptors sense the presence of germinants.[26] Together, sporulation, germination, and outgrowth of vegetative cells in the gut are central to the vicious infection cycle of *C. difficile*, which is difficult to break with existing antibiotics.

Natural products derived from microbes are the most important source of antibiotic lead compounds and of antimicrobials with new types of activities.[27] Chlorotonil A (ChA) is a polyketide isolated from the myxobacterium *Sorangium cellulosum* with strong antibacterial activity against Gram-positive bacteria and moderate antifungal activity.[28,29] Moreover, it exhibits bioactivity against the malaria-causing pathogen *Plasmodium falciparum*.[30] A derivate of ChA, ChB1-Epo2, was recently generated by introducing an epoxide bond and removing a chlorine atom to improve the limited aqueous solubility, as well as *in vivo* stability and systemic bioavailability, respectively.[31] Due to their antibacterial activity being restricted to Gram-positive pathogens, we reasoned that chlorotonils are good candidates to clear infections caused by *C. difficile* with less drastic effects on the gut microbiome compared with vancomycin. Furthermore, no cross-resistance with other antibiotics has been reported so far,[31] making ChA a good candidate as an antibacterial agent.

RESULTS

Chlorotonils show antimicrobial activity against diverse *C. difficile* strains

Here, we investigated the effectiveness and potential antimicrobial activity of ChA and its semisynthetic derivative ChB1-Epo2 (Figures 1A and 1B) against *C. difficile*. To cover the broad genomic diversity of this pathogen, the screening panel included the well-characterized *C. difficile* strains 630, VPI10463, DSM 1296 (typestrain), R20291, and strains resistant against metronidazole (CD-22-00115) or fidaxomicin (CD-22-00001), or with reduced susceptibility to vancomycin (CD-10-00484 and CD-15-00638). Strains were screened in standardized liquid broth dilution assays using ChA and ChB1-Epo2 in decreasing concentrations (6.4 μg/mL to 3.125 ng/mL) to determine the minimum inhibitory concentration (MIC) and the minimum bactericidal concentration (MBC).

In line with our expectations, the four antibiotic-resistant/resilient strains showed increased MIC/MBC values compared with the strains without resistance or with resistance against other antibiotics (Figure 1C). In contrast, both chlorotonils exhibited MIC and MBC values comparable with or superior to vancomycin (0.4–0.8 μg/mL), ranging between 0.4–1.6 μg/mL for ChA and 0.05–0.2 μg/mL for ChB1-Epo2, with differences based on strain and antibiotic (Figures 1B and 1C). Strains resistant against either metronidazole or fidaxomicin, or with reduced susceptibility to vancomycin, displayed comparable sensitivity with chlorotonils, indicating the absence of cross-resistance between the antibiotics. Based on the classical definition of bactericidal antibiotics, i.e., a ratio of MIC to MBC < 4, we classified both chlorotonils as bactericidal.

ChB1-Epo2 forces metabolic reprogramming and disturbed metal homeostasis at sublethal concentrations

To further address physiological and biochemical alterations at sublethal concentrations, we investigated the transcriptional response of *C. difficile* strain 630, one of the best characterized isolates in terms of regulon and metabolic network structures.[32] We decided to focus on ChB1-Epo2 as both chlorotonils had a similar pattern of inhibition between strains (Figures 1B and 1C), yet with a higher activity of ChB1-Epo2. Specifically, *C. difficile* was grown to mid-exponential phase and stressed for 30 min with 4.7 ng/mL of ChB1-Epo2, a sublethal concentration inducing significant growth delay. DMSO-treated cells served as control. Of the 3,774 detected genes, 213 transcripts were significantly less abundant ($\log_2$fold change [FC] ≤ -1.0), and 207 transcripts were significantly more abundant ($\log_2$FC ≥ 1.0), in comparison with the control. A large number of upregulated genes belong to the categories of energy production and conversion and to cell-wall biogenesis (Figure 2A). We found transcripts of *prdAB*, which encode the proline reductase, to be more abundant in stressed cells. Furthermore, induced genes encode phosphotransferase systems and enzymes that are presumed to be involved in the uptake and utilization of alternative carbohydrates. In addition, we observed induction of typical stress responses of *C. difficile*, characterized by genes that encode a CcmA-like drug resistance transporter, a putative superoxide reductase, a pyrimidine dimer repair enzyme, carbon starvation protein CstA, and a sporulation factor. On the other hand, transcript levels of genes responsible for the biosynthesis of macromolecules such as fatty acids, the formation of cellular structures such as flagella, and purine biosynthesis were reduced. In brief, the response of the pathogen to ChB1-Epo2 was mainly characterized by a drastic reprogramming of the

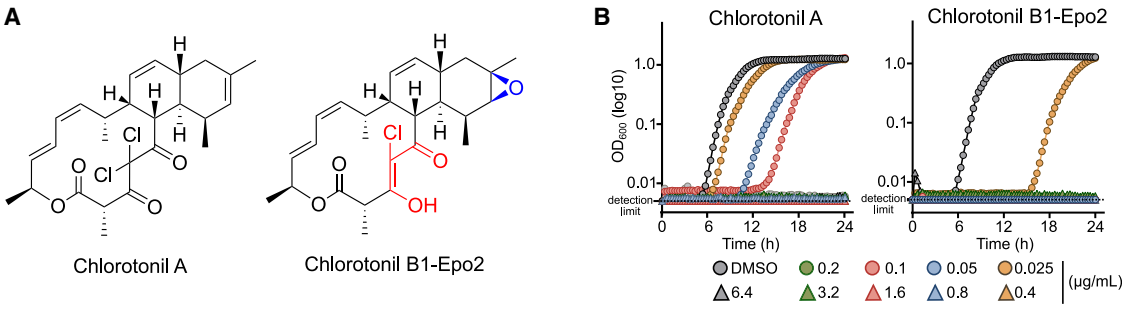

C

	ChA		ChB1-Epo2		Vancomycin		Metronidazole		Fidaxomicin	
***C. difficile* strain**	**MIC**	**MBC**	**MIC**	**MBC**	**MIC**	**MBC**	**MIC**	**MBC**	**MIC**	**MBC**
630	0.4	0.8	0.05	0.1	0.4	0.8	0.4	0.8	0.00625	0.05
VPI 10463	0.4	0.4	0.05	0.05	0.8	0.8	0.8	0.8	0.00625	0.05
1780	0.8	0.8	0.1	0.1	0.4	0.4	0.2	0.4	0.0125	0.1
R20291	1.6	1.6	0.1	0.2	0.8	0.8	0.4	0.8	0.0125	0.2
CD-10-00484 (**V1**)	0.8	0.8	0.2	0.2	3.2	>6.4	0.4	0.8	0.00625	0.1
CD-22-00115 (**M1**)	0.4	0.4	0.2	0.1	0.8	0.8	>6.4	>6.4	0.00312	0.05
CD-22-00001 (**F1**)	0.4	0.4	0.2	0.2	0.8	0.8	0.1	0.2	>3.2	>3.2
CD-15-00638 (**V2**)	0.8	0.8	0.1	0.1	6.4	>6.4	0.8	0.8	0.00625	0.05

*values are depicted in μg/mL
**V1, V2 = vancomycin resilient; M1 = metronidazole resistant; F1 = fidaxomicin resistant

Figure 1. Chlorotonils show antimicrobial activity against *C. difficile*

(A) Chemical structures of ChA and the semisynthetic, epoxidized derivative ChB1-Epo2.

(B) *C. difficile* strain VPI10463 growth curves in the presence of increasing concentrations of ChA (left) and ChB1-Epo2 (right). Dotted line represents detection limit.

(C) MIC and MBC of ChA, ChB1-Epo2, vancomycin, metronidazole, and fidaxomicin against a panel of *C. difficile* strains.

energy, AA, and carbohydrate metabolism, a decrease in macromolecule and polyamine synthesis, and an increased abundance of stress-response-related gene transcripts (Figure S1; Table S1).

To complement this approach, the proteome of *C. difficile* 630 after 90 min of growth in the presence of the same sublethal dose of ChB1-Epo2 (4.7 ng/mL) was analyzed by LC-MS/MS, resulting in the identification of 1,513 proteins with 62 proteins being significantly more or less abundant after stress. Of those, three proteins were significantly more abundant, and 29 proteins were identified exclusively in ChB1-Epo2-stressed cells ("ON" proteins). In contrast, one protein was significantly less abundant, and 29 proteins were identified exclusively in the DMSO controls but not in ChB1-Epo2-stressed cells ("OFF" proteins). Of the 32 higher abundant and ON proteins, eleven are predicted to bind transient metals or iron-sulfur clusters on their conserved cysteine motives (Table S2). The large number of metal-containing proteins affected by the presence of ChB1-Epo2 led us to hypothesize that ChB1-Epo2 caused a disturbance in metal homeostasis. To investigate this hypothesis, we analyzed the metal content of cells treated with ChB1-Epo2 and untreated cells using inductively coupled plasma-mass spectrometry (ICP-MS) analysis. The ICP-MS results demonstrated a significant increase in the divalent cations copper, zinc, and cadmium (Figure 2C).

In summary, these complementary approaches reveal the disturbance of key metabolic functions of *C. difficile* by ChB1-Epo2, even at sub-MIC concentrations, and provide directions for future mode-of-action studies.

ChA successfully antagonizes established CDI and prevents relapsing infection

Next, we assessed the potential of chlorotonils for treating CDI. To this end, we applied a well-established infection model based on clindamycin-induced disruption of the microbiota.[33] Briefly, after clindamycin pre-treatment, specific pathogen-free (SPF) mice were infected with 10^4 spores of *C. difficile* VPI10463 (day 0) (Figure 3A). This strain is commonly used for mouse infection studies[34] and susceptible to vancomycin, ChA, and ChB1-Epo2. On the two following days (day 1 and 2), infected mice were treated with 40 mg/kg ChA, 40 mg/kg ChB1-Epo2, or 20 mg/kg vancomycin (Figure 3A). Antibiotic treatment was discontinued after day 2 to monitor the durability of the antimicrobial effect and to allow the potential development of a relapsing infection. As expected, 24 h post infection (day 1), mice suffered from severe weight loss (Figure 3B), indicating a rapid onset of the disease. Strikingly, in the days after the second dose, most vancomycin- and ChA-treated mice of both groups started to recover to a final survival rate of 66.6% (6/9 mice). Surprisingly, ChB1-Epo2-treated mice started to succumb to the infection,

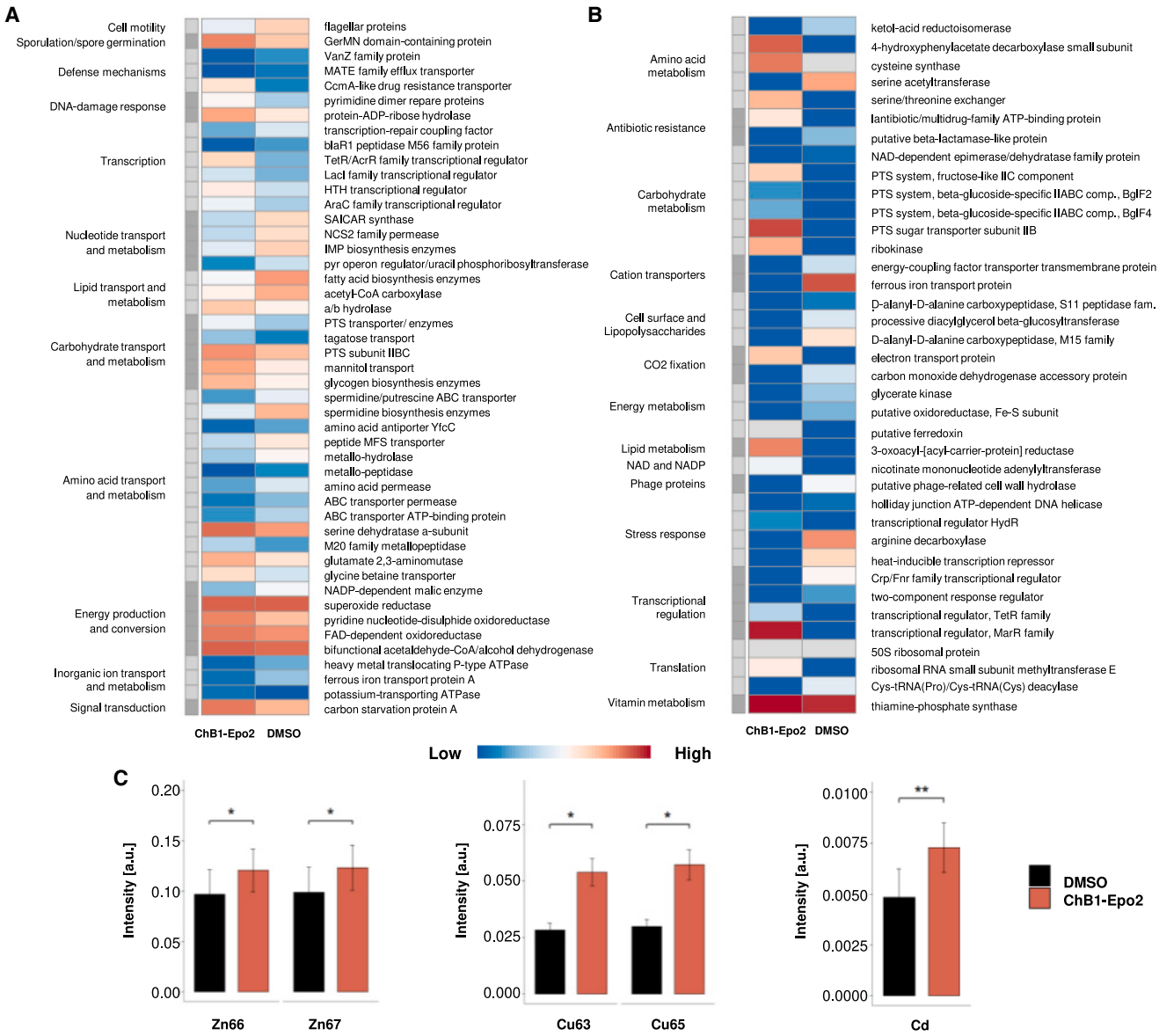

Figure 2. ChB1-Epo2 forces metabolic reprogramming and disturbed metal homeostasis at sublethal concentrations

(A–C) The stress response signature of *C. difficile* 630 to a sublethal dose ChB1-Epo2 (4.7 ng/mL) was analyzed on transcriptome level 30 min after treatment (A), as well as 90 min after treatment on proteome level (B) and ICP-MS analysis of intracellular metal concentrations (C).

(A) Transcripts that were differentially abundant between stressed and DMSO-treated cells with a $\log_2$FC of at least 1.5 were mapped on a heatmap displaying *C. difficile*'s gene inventory clustered according to the functional role of the respective proteins. The number of gene transcripts per million are scored in colors. Proteins and functional categories are indicated.

(B) 62 proteins were differential abundant and were either significantly higher abundant ($\log_2$FC $\geq$ 1.5) or only identified in ChB1-Epo2-stressed cells compared with the DMSO controls, or vice versa. Protein abundances are scored in colors.

(C) Intracellular concentrations of zinc, copper, and cadmium. Error bars represent mean ± standard deviation (s.d.). (*$p < 0.05$, **$p < 0.01$).

See also Figure S1 and Tables S1 and S2.

resulting in a final survival rate of 22.2% (2/9 mice), identical to that of the vehicle-treated control group (Figure 3C). After the initial recovery of vancomycin-treated mice, they started to lose weight again, likely as a result of a relapsing infection (Figures S2A and S2B). In contrast, ChA-treated mice steadily recovered their weight without an observable disease relapse. Although vancomycin-treated mice demonstrated a faster weight recovery than ChA-treated mice early on, we did not observe significant differences in *C. difficile* numbers between the two groups at day 3 (Figure 3D). The relapsing phenotype observed in the vancomycin treatment group on day 5 was characterized by significantly higher numbers of *C. difficile* vegetative cells and spores compared to the ChA treatment group, indicating that ChA treatment more efficiently clears *C. difficile* after severe infection. In fact, 83.3% of surviving mice (5/6) in the ChA treatment group compared with 16.6% (1/6) in the vancomycin

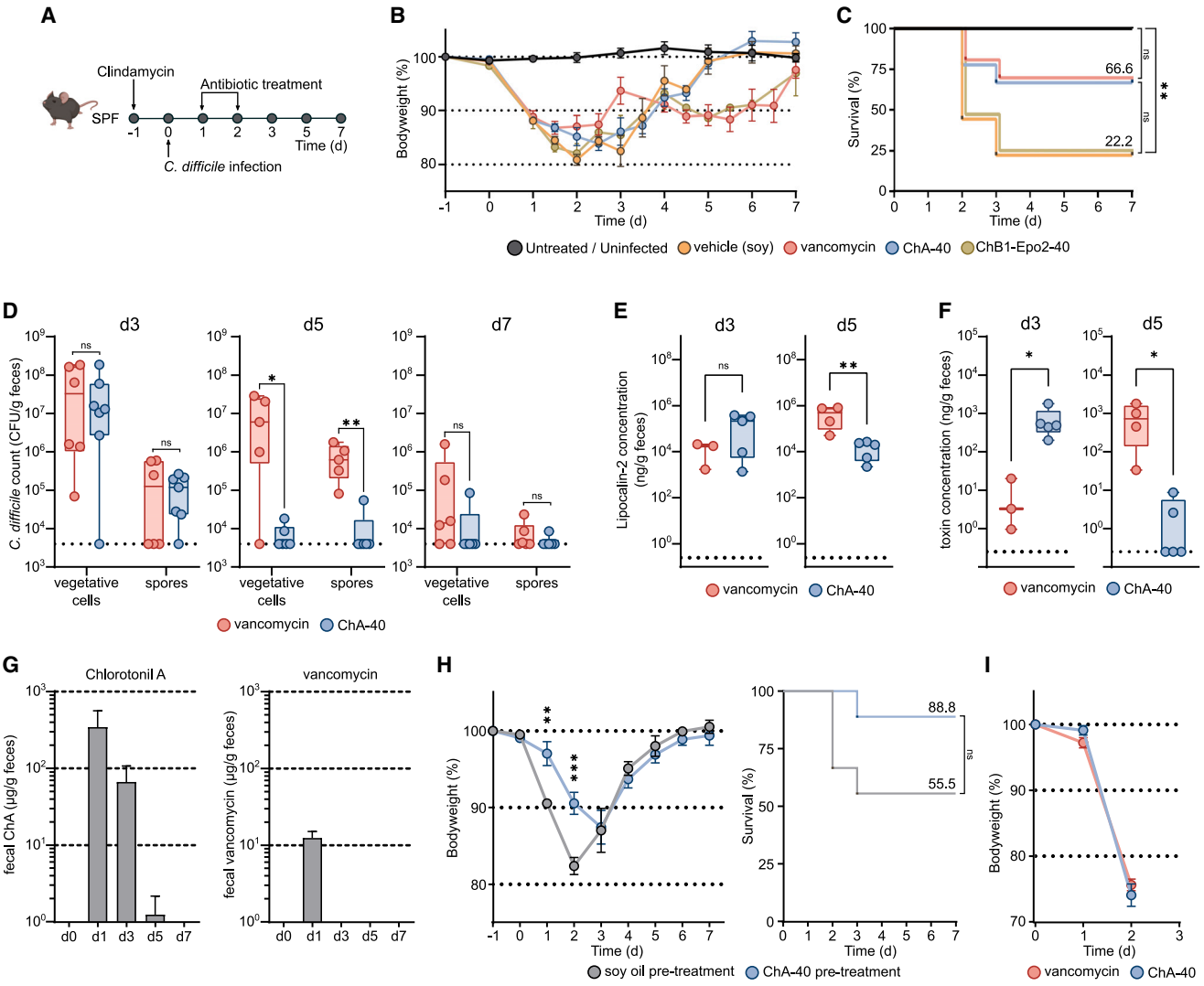

Figure 3. ChA successfully antagonizes established CDI and prevents relapsing infection

(A–F) SPF mice (n = 9/group) were pre-treated with clindamycin (10 mg/kg) (day −1) and infected with 10^4 spores of VPI10463 (day 0), followed by antibiotic treatment (day 1 and 2).

(B) Average daily body weight of infected or uninfected/untreated mice.

(C) Kaplan-Meier survival curves of infected mice, p values were determined using a log-rank (Mantel-Cox) test.

(D) Fecal burden of *C. difficile* spores and vegetative cells at different time points of infection. The dotted lines represent the detection limits.

(E and F) Lipocalin-2 and total *C. difficile* toxin (TcdA and TcdB pooled) ELISA from fecal samples. p values in (D)–(F) represent Mann-Whitney non-parametric rank comparison between ChA and vancomycin treatment.

(G) Quantification of ChA (left) and vancomycin (right) from fecal samples at different time point before (day 0) and after (day 1, 3, 5, and 7) treatment with ChA (40 mg/kg) and vancomycin (20 mg/kg) (n = 5–8/day/antibiotic).

(H) SPF mice (n = 9/group) were pre-treated with clindamycin (10 mg/kg) and either ChA (40 mg/kg) or soy oil (day −1) and infected with 10^4 spores of VPI10463 (day 0). Left: average daily weight of infected mice. p values represent Mann-Whitney non-parametric rank comparison between treatments at the days indicated. Right: Kaplan-Meier survival curves.

(I) GF mice (n = 7/group) were infected with 10^3 spores *C. difficile* VPI10463 followed by antibiotic treatment at day 1 p.i. Average daily body weight of infected GF mice. Error bars represent ± standard errors of the mean (SEM). (*p < 0.05, **p < 0.01, ***p < 0.0001).

See also Figure S2.

treatment group cleared *C. difficile* completely until day 7 (Figure S2C), i.e., vegetative cells and spores were absent in the feces of these mice (Figure 3D). Comparison of the levels of lipocalin-2, a marker of intestinal inflammation, revealed significant differences at day 5, the time point when the weight difference first became detectable again (Figure 3E). Moreover, while vancomycin-treated mice exhibited lower levels of toxins at day 3, we observed an approximately 100-fold reduced amount of toxins detected in ChA-treated mice compared with vancomycin-treated mice at day 5 (Figure 3F).

Since vancomycin and ChA have comparable antimicrobial effects *in vitro*, we hypothesized that other factors, such as

CellPress
OPEN ACCESS

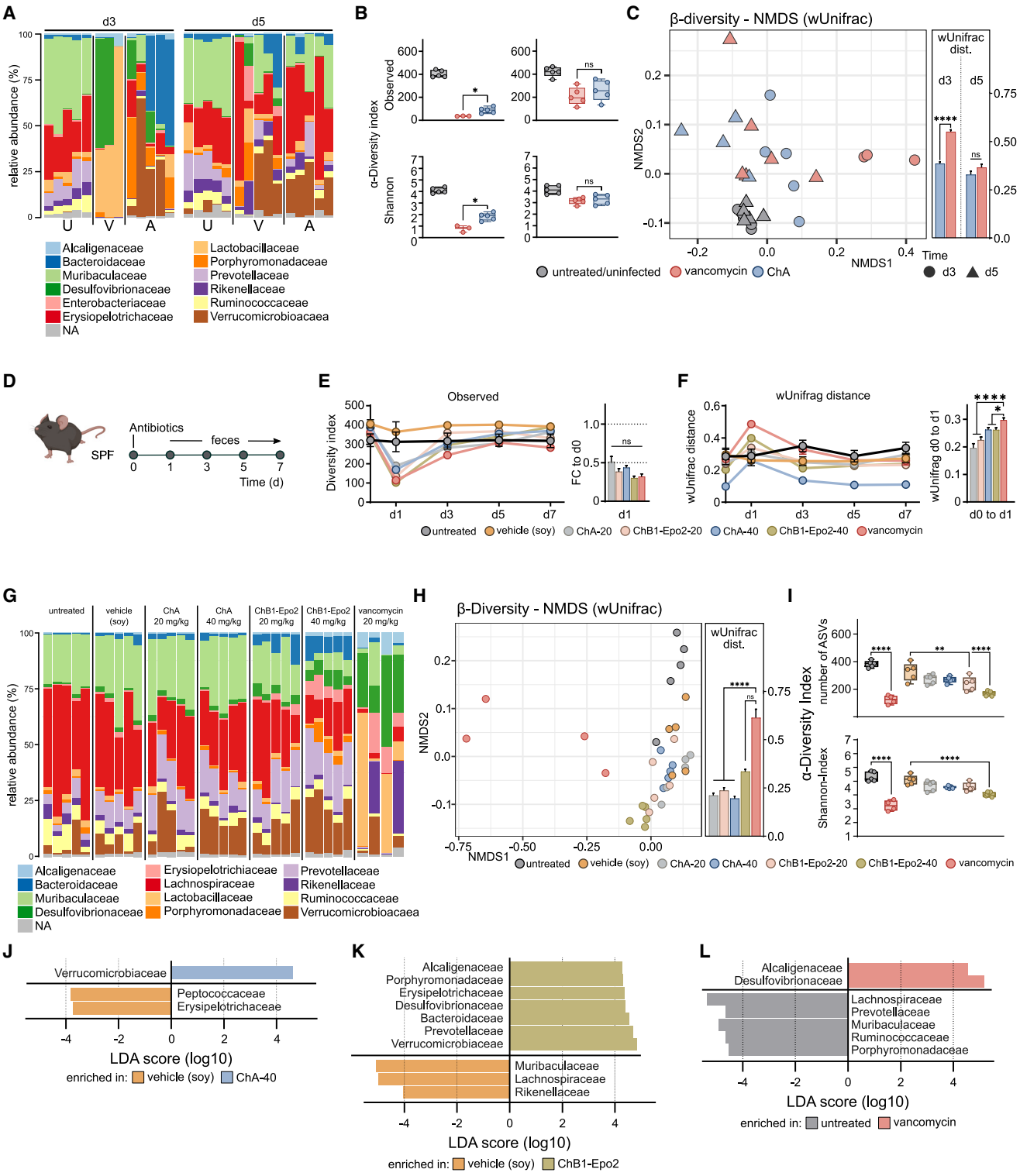

Figure 4. In mice, ChA induces distinct microbiota changes compared with ChB-Epo2 and vancomycin

(A and B) Changes in colonic microbiota composition and α-diversity at days 3 and 5 p.i. of infected and ChA or vancomycin treated mice. Untreated and uninfected mice were used as controls (n = 3–5/group).

(A) Single sample relative abundance (%) of 12 most abundant bacterial families; U, untreated/uninfected; V, vancomycin; A, ChA.

(B) Quantification of α-diversity from the fecal microbiota using observed species richness (amplicon sequencing variants, ASVs) and Shannon index.

(legend continued on next page)

antibiotic transit time or microbiota-mediated CR, contributed to efficient clearance of *C. difficile* from ChA-treated mice. Hence, we longitudinally quantified antibiotic concentrations in fecal samples of ChA- and vancomycin-treated SPF mice. Higher levels of ChA were detected in comparison with vancomycin on day 1 post treatment (Figure 3G). Specifically, although ChA was administered at a 2-fold higher concentration than vancomycin, approximately 25-fold higher concentrations of ChA than of vancomycin were detected. Furthermore, concentrations of vancomycin were below the limit of detection on the following days, whereas ChA was still detected on day 3 and 5, yet at 10- to 500-fold lower concentrations compared with day 1. To test whether the persisting ChA levels are sufficient to modulate CDI development *in vivo*, we pre-treated SPF mice with clindamycin (10 mg/kg) and ChA (40 mg/kg) or soy oil (as control), followed by CDI. Strikingly, ChA pre-treatment resulted in significantly slower onset of disease and minor severity compared with the control, characterized by reduced weight loss and higher survival rates (Figure 3H). These results indicate that persisting ChA is able to antagonize *C. difficile* for an extended period, which may promote clearance. To evaluate whether the presence of a regenerating microbiota is critical for treatment outcome, the therapeutic effects of ChA and vancomycin were assessed in the absence of a healthy microbiota, i.e., by infecting germ-free (GF) mice with *C. difficile* followed by antibiotic treatment starting on day 1 post infection (p.i.). Strikingly, we observed severe bodyweight loss regardless of treatment (Figure 3I), resulting in mortality rates of 100% (7/7) on day 2 p.i. Thus, neither ChA nor vancomycin were able to successfully prevent CDI in GF mice, suggesting a physiologically relevant contribution of a recovering microbiota in the successful treatment of CDI.

In mice, ChA induces distinct microbiota changes compared with ChB-Epo2 and vancomycin

To test the hypothesis that ChA and vancomycin have distinct impacts on microbiota composition, which, in turn, may be associated with the better clearance of *C. difficile* from ChA-treated mice, we performed microbiota analysis of luminal colon samples from the infection experiments. Infected and ChA-treated mice revealed strong differences at day 3 in their microbiota composition compared with that of vancomycin-treated mice (Figure 4A). Specifically, the more diverse microbiota of ChA-treated mice featured members of the Porphyromonadaceae, Verrucomicrobiaceae, and Bacteroidaceae, i.e., families of Gram-negative bacteria that may contribute to better clearance of *C. difficile*.[35] Notably, due to the prior clindamycin treatment and the *C. difficile*-induced inflammation, both communities were distinct to the one in the untreated and uninfected group of mice at day 3 p.i. However, we observed significant differences in α-diversity (Figure 4B), as well as weighted unifrac (wUnifrac) distance, i.e., the measure of phylogenetic distances[36] in β-diversity (Figure 4C) between ChA- and vancomycin-treated mice at day 3, indicating a faster microbiota recovery after ChA treatment. At day 5, the differences between treatments were less pronounced. However, levels of Muribaculaceae, Lachnospiraceae, and Verrucomicrobiaceae members were still noticeably distinct compared with uninfected and untreated mice (Figure 4A).

Next, we addressed the question whether vancomycin, ChA, and ChB1-Epo2 treatment in the absence of any pre-treatment and infection have similar or distinct effects on the intestinal microbiota. To this end, mice were treated with a single oral dose of either ChA or ChB1-Epo2 at two concentrations (40 and 20 mg/kg) (Figure 4D). Feces samples were collected longitudinally from the same mice at different time points (day 0, 1, 3, 5, and 7) and subjected to 16S rRNA gene sequencing. As expected, a strong impact of vancomycin was observed on the microbiota, significantly reducing the observed species richness, and on the Shannon diversity index 24 h post treatment (Figures 4E and S3A), followed by a slow recovery within 1 week. Similarly, ChA and ChB1-Epo2 reduced the observed species richness and Shannon diversity index transiently (Figures 4E and S3A). No differences were observed in the Shannon diversity index (Figure S3A). After performing β-diversity analysis, we calculated wUnifrac distances of the longitudinal dataset compared with their initial state (day 0). This revealed that on day 1, vancomycin had a stronger effect (mean dist. = 0.29), compared with the higher concentrations of ChB1-Epo2 (0.26) and ChA (0.26), respectively (*$p < 0.05$) (Figure 4F). Starting on day 3, no significant differences in the wUnifrac distances were detected between the groups. This trend was also visible in the non-metric multidimensional scaling (NMDS) analysis, showing distinct clustering of vancomycin- and ChB1-Epo2-treatment 24 h post treatment, which converges with the control and ChA samples starting from day 3 onward (Figure S4B). Characterization of the microbiota changes on the family level illustrated that distinct groups of commensal bacteria were temporarily affected by the antibiotics (Figure S4C).

In addition to the longitudinal analysis from fecal samples, cecal samples were analyzed 24 h post treatment. Vancomycin treatment again resulted in the largest changes with an expansion of normally rare microbes such as Desulfovibrionaceae

(C) NMDS plot showing β-diversity using wUnifrac distances. Centroid wUnifrac distances (right) were calculated between each untreated/uninfected sample and each antibiotic sample at specified day. p values in (B) and (C) represent Mann-Whitney non-parametric rank comparison between ChA- and vancomycin treatment.

(D–F) Longitudinal microbiota analysis of fecal samples after antibiotic treatment in SPF mice (n = 4–5/group). (E and F) Quantification of longitudinal changes in (E) α-diversity using observed species richness (ASVs) and (F) β-diversity using wUnifrac distance after antibiotic treatment (day 0). Barplots (right) represent pairwise (E) fold change and (F) wUnifrac distance calculated between day 0 and 1 values for each mouse, respectively.

(G–L) Microbiota analysis of cecal samples 24 h after antibiotic treatment in SPF mice (n = 4–5). (G) Single sample relative abundance (%) of 12 most abundant bacterial families. (H) NMDS plot showing β-diversity using wUnifrac distances. Centroid wUnifrac distances (right) were calculated between each antibiotic sample and each sample of their respective control group sample (vancomycin-untreated; chlorotonils-soy oil). (I) Quantification of α-diversity from the cecal microbiota using observed species richness (ASVs) and Shannon index.

(J–L) Comparison of changes in the cecal microbiota after (J) ChA, (K) ChB1-Epo2, and (L) vancomycin treatment on family level by linear discriminant analysis (LDA) effect size (LEfSe). p values in (E)–(I) represent Kruskall-Wallis tests between all antibiotic treatments. Error bars represent ± SEM. (*$p < 0.05$, **$p < 0.01$, ****$p < 0.0001$).

See also Figure S3 and Table S3.

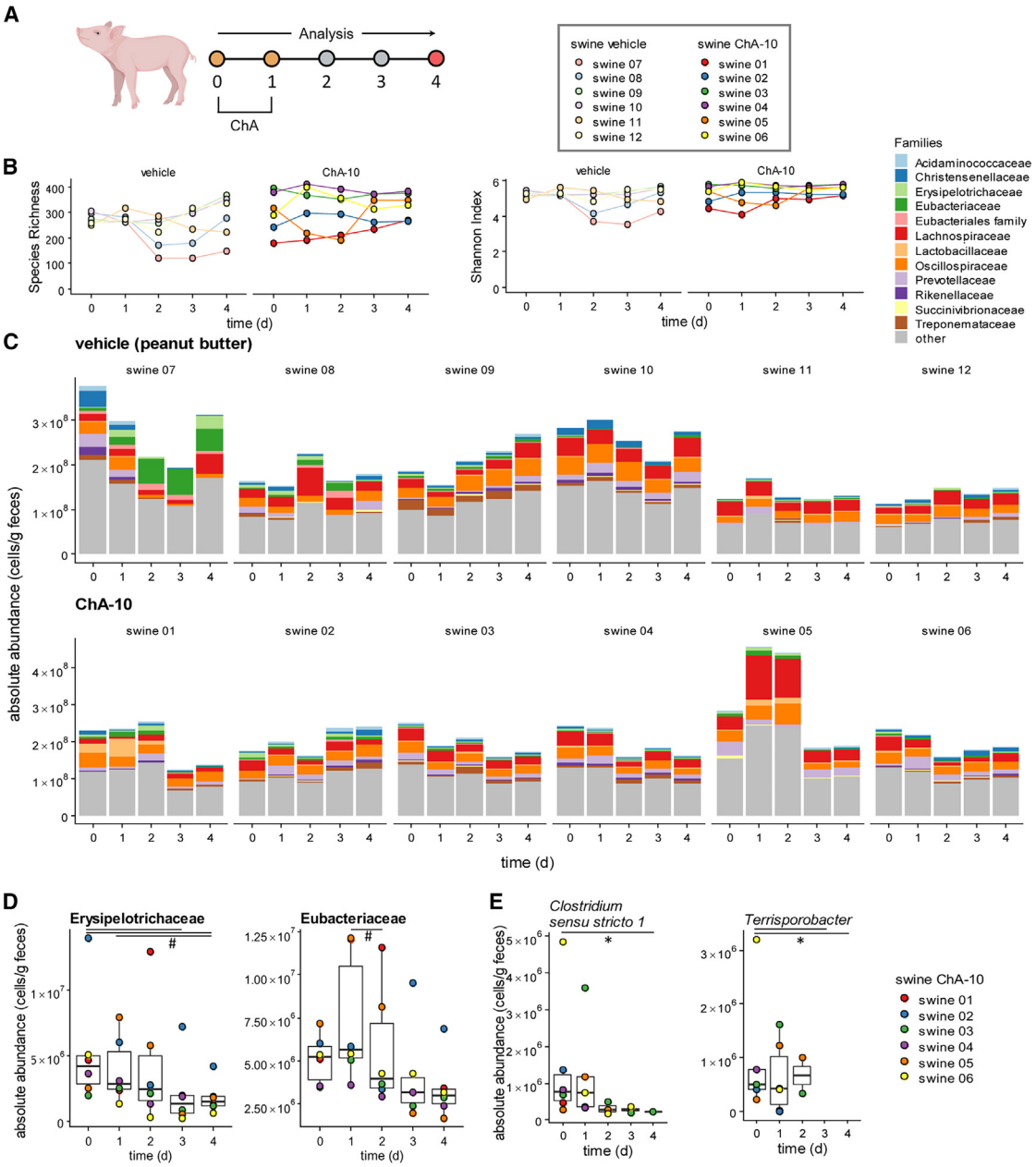

Figure 5. ChA has minor effects on the piglet microbiota

(A) Scheme of the piglet experiment to monitor changes in the cecal microbiota of piglets before (day 0) and after antibiotic treatment (day 1, 2, 3, and 4).

(B) Quantification of α-diversity by species richness and Shannon index (n = 6/group).

(C) Absolute abundance (cells/g feces) of the 12 most abundant bacterial families, depicted for piglets separately. Significantly changed genera are in boxplots for the control group and the ChA-treated group. p values were calculated between respective days (*p < 0.05 paired Wilcoxon signed rank sum test, *p < 0.05 pairwise Fisher's exact test).

(D and E) (D) Families and (E) genera with significantly changed absolute abundance (cells/g feces) shown in boxplots for the ChA-treated group.

See also Figure S4 and Tables S4 and S5.

(Figure 4G; Table S3). Compared with the control group, ChA and ChB1-Epo2 led to a partial reduction in the Lachnospiraceae family abundance (relative abundance in soy oil, 36%; ChA, 28.8%; ChB1-Epo2, 15.9%; and vancomycin, 2.7%), whereas ChB1-Epo2 and vancomycin also reduced the abundance of the family Muribaculaceae in a dose-dependent manner (soy oil, 29.0%; ChA, 28.5%; ChB1-Epo2, 6.0%; and vancomycin, 6.4%). Analysis of β-diversity and calculation of wUnifrac distances corroborated the distinct impact of the antibiotics on the microbiota and a stronger effect of vancomycin (mean dist. = 0.61), compared with ChB1-Epo2 (0.33, p = 0.12) or ChA (0.10, ****p < 0.0001) (Figure 4H). In line with this observation, significant changes in

α-diversity were only detected after treatment with ChB1-Epo2 and vancomycin (Figure 4I), compared with their respective control group (****$p < 0.0001$). Next, microbiota changes after chlorotonil and vancomycin treatments were analyzed on family level by linear discriminant analysis (LDA) effect size (LEfSe). For ChA, changes were mainly observed in levels of Verrucomicrobiaceae (increased), Peptococcaceae, and Erysipelotrichaceae (both decreased) (Figure 4J). ChB1-Epo2 treatment led to a reduction of Lachnospiraceae, Rikenellaceae, and Muribaculaceae but to an increase in several bacterial families, including Bacteroidaceae, Prevotellaceae, and Verrucomicrobiaceae, representing major Gram-negative phyla of the mouse gut microbiome (Figure 4K). Vancomycin induced similar changes to ChB1-Epo2, while simultaneously increasing Desulfovibrionaceae and Alcaligenaceae (Figure 4L).

Taken together, these results provide evidence that ChA treatment results in faster microbiota recovery during CDI compared to vancomycin and that a single dose of ChA induces distinct and less severe changes to the microbiota, compared with ChB1-Epo2 or vancomycin.

ChA has minor effects on the piglet microbiota

To corroborate the effect of chlorotonils on the murine microbiota, we performed a feeding trial with pigs, a model with more similarities in genetics, physiology, and microbiota composition to humans compared with rodents.[37] A peanut butter formulation with and without ChA was fed to 6-week-old piglets (20 mg/kg, n = 6/group twice within an interval of 24 h) (Figure 5A). From each animal, fecal samples were taken before (day 0) and 6 h after the second antibiotic treatment (day 1), as well as on the following 3 days (day 2, 3, and 4). Notably, no significant changes were found over time in the α-diversity of the fecal samples (Figure 5B), but a higher inter-individual variability between piglets as compared with mice was observed, although values largely recovered until the end of the experiment.

Next, absolute abundances were determined via flow cytometry, and quantitative bacterial cell numbers significantly varied between samples, individuals, and time points, even in the control group (Figure 5C). For instance, piglet 01 exhibited a reduction in bacterial cells of 50% per gram feces from day 2 to day 3. Despite the variation in initial cell numbers of Lactobacillaceae, we observed a reduction of this family across all ChA-treated animals (Figure 5D). Regardless of the high inter-individual variability of the microbiota composition, the abundance of Erysipelotrichaceae was significantly decreased in ChA-treated piglets at day 3 and 4 compared with day 0, along with a significant reduction of Eubacteriaceae ChA-treated piglets at day 2 as compared with day 1. No other changes on the family level were detected (Tables S4 and S5). Analysis on the genus level revealed only two out of the 138 detected genera to be significantly decreased following ChA treatment. The genus *Clostridium sensu stricto 1* decreased at day 4, and that of the genus *Terrisporobacter* at day 3 and 4, respectively (Figure 5E), both, similar to *C. difficile*, belonging to the Peptostreptococcaceae family.

In light of the minor impact of ChA on the porcine microbiota, we assessed whether ChA is detectable and biologically active in the porcine fecal samples. We found ChA until day 3 with the highest concentrations on day 1 and 2 (Figure S4A). The bioactivity of ChA was evaluated by cultivation of the ChA-sensitive indicator strain *Stapylococcus aureus* in LB medium with different concentrations (10% and 25%) of fecal samples from control or ChA-treated animals. Growth of *S. aureus* was inhibited in the presence of diluted feces from treated, but not from control animals (Figures S4B and S4C).

Together, these data reveal that in the porcine microbiota, some groups of Gram-positive bacteria are affected by ChA, but that these effects are transient, with the exception of the two closely related genera *Terrisporobacter* and *Clostridioides*. Hence, similar to the mouse model, ChA treatment caused only minor effects on the composition of the diverse microbiomes of piglets without influence on α-diversity and cell densities.

Chlorotonil treatment sustains intestinal metabolism and preserves the natural CR against *C. difficile*

Since antibiotic treatment has distinct effects on the murine microbiota composition and thus potentially on the functionality of the microbiota, we quantified metabolites contributing to CR against *C. difficile*.[15,38,39] For total BAs, a significant reduction (>10-fold) was observed in clindamycin- and vancomycin-treated mice, but not after ChA or ChB1-Epo2 treatment (Figures S5A and S5B). Clindamycin and vancomycin treatment reduced the abundance of *C. difficile*-inhibiting secondary BAs (deoxycholic acid [DCA], lithocholic acid [LCA], and omega-muricholic acid [ω-MCA]) up to 100- to 1,000-fold, respectively (Figure 6A). Although variations in individual BAs were detected, we did not observe a significant change in the levels of DCA, LCA, ω-MCA, and ursodeoxycholic acid (UDCA) between ChA- and ChB1-Epo2 treatment and the respective controls (Figures 6A and S5B). Notably, these experiments did not reveal distinctions between ChA and ChB1-Epo2, despite their different impact on microbiota composition. In contrast, the effect of vancomycin in comparison with ChA on the BA metabolism became evident, which may help to explain differences in observed rCDI. Hence, we quantified primary, deconjugated, and secondary BAs at day 3 and 5 after CDI and treatment with vancomycin and ChA (Figure 3A). As expected, we observed a strong change in *C. difficile*-inhibiting BAs (LCA, DCA, iso-DCA, chenodeoxycholic acid [CDCA], UDCA, ω-MCA) between uninfected mice and *C. difficile*-infected and treated mice (Figure S5C). A trend toward higher concentrations of *C. difficile*-inhibiting BAs was observed in ChA- compared with vancomycin-treated mice; however, it was not significant. Since mice were pre-treated with clindamycin in this experiment to enable *C. difficile* colonization, we conclude that the intestinal BA pool remains severely disrupted regardless of subsequent vancomycin or ChA treatment and consequently does not explain the difference in rCDI.

Since nutrient competition and Stickland fermentation similarly contribute to CR against *C. difficile*,[17,40] we quantified an additional panel of metabolites consisting of AAs, short-chain fatty acids (SCFAs), and Stickland-metabolites from fecal samples at baseline (day 0) and 24 h post (day 1) ChA, vancomycin, or clindamycin treatment. The analysis revealed that all three antibiotics induce changes in metabolite concentrations. However, the sample cluster formed by ChA treatment is closest to all baseline samples as quantified by NMDS based on Euclidean distance (Figures 6B and S5D). Specifically, mean distances between day 0 and 1 samples are significantly (*$p < 0.05$) lower after ChA treatment (dist: 0.04) compared with clindamycin

CellPress
OPEN ACCESS

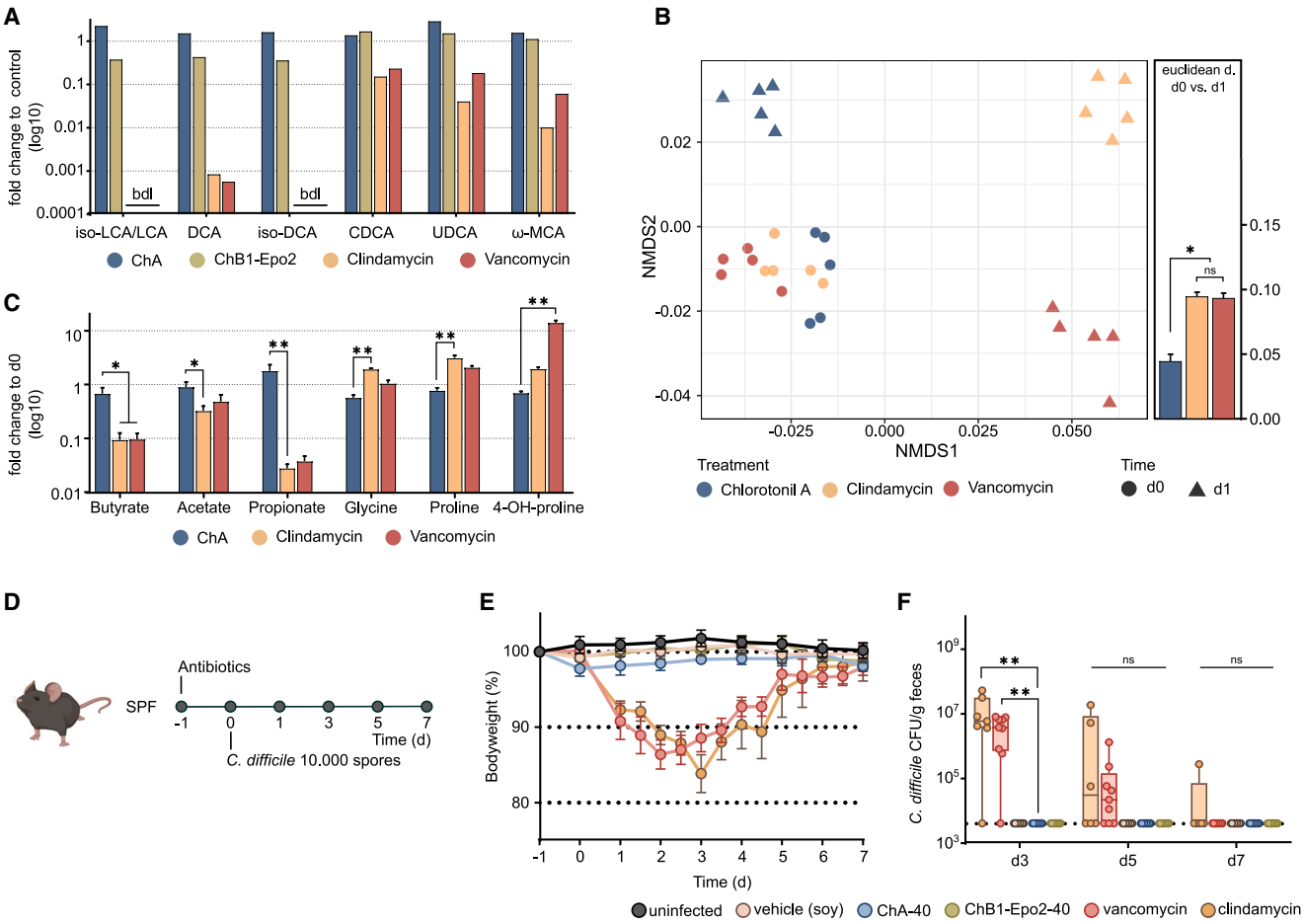

Figure 6. Chlorotonil treatment sustains intestinal metabolism and preserves the natural CR against *C. difficile*

(A) Targeted quantification of colonic bile acids 24 h after antibiotic treatment. Fold-change of *C. difficile*-inhibiting bile acids per treatment, calculated to respective control samples (vancomycin and clindamycin versus untreated; chlorotonils versus soy oil); (n = 4–5/group). Concentrations of iso-LCA/LCA and iso-DCA post clindamycin and vancomycin treatment were below detection limit (bdl).

(B and C) Targeted quantification of *C. difficile*-associated metabolites from fecal samples of mice 24 h post treatment with ChA (40 mg/kg), clindamycin (10 mg/kg) or vancomycin (20 mg/kg); (n = 5/group).

(B) Non-metric multidimensional scaling (NMDS) using Euclidean distance across all detected metabolites, depicted at baseline (day 0) and 24 h post antibiotic treatment (day 1). Pairwise Euclidean distances were calculated between each baseline sample and their respective treatment sample.

(C) Pairwise fold-change of specified metabolites calculated between each baseline (day 0) and treatment (day 1) sample, respectively.

(D–F) SPF (n = 9/group) mice were pre-treated with antibiotics (day −1) and infected with 10^4 spores VPI10463 (day 0).

(E) Average daily weight of infected or untreated/uninfected mice.

(F) Fecal burden of *C. difficile* spores and vegetative cells (pooled) at different infection time points. p values in (C) and (F) represent Kruskall-Wallis one-way ANOVA calculated between treatments. Error bars represent ± SEM. (*p < 0.05, **p < 0.01).

See also Figure S5.

(dist: 0.094) and vancomycin (dist: 0.092). In particular, SCFAs, which have been shown to induce protection from *C. difficile*,[39] are significantly reduced following clindamycin or vancomycin treatment, whereas concentrations following ChA-treatment remained largely unchanged (Figure 6C). Additionally, we observe increased concentrations of proline, 4-hydroxyproline, or glycine after vancomycin or clindamycin, but not ChA treatment. These two metabolites are essential for reductive Stickland-metabolism, and their availability in the intestinal tract promote *C. difficile* colonization and disease outbreak.[41,42] In turn, Stickland metabolites have been associated with protection against *C. difficile*, reflecting the presence of metabolically related bacteria in the intestine.[17] Following ChA treatment, most of the detected Stickland products, except 5-aminovalerate and indole-3-acetate, remain unchanged or are elevated (Figure S5D). In contrast, clindamycin and vancomycin treatment strongly influenced the output of these specific metabolites, suggesting a stronger impact on Stickland fermentation, thereby providing a favorable nutritional niche for *C. difficile*. Together, these results demonstrate that ChA treatment has a lower impact on the intestinal metabolome compared with vancomycin or clindamycin treatment. Thus, we speculated that the nutritional niche of *C. difficile* remains occupied after ChA treatment; therefore, CR against CDI should still be intact.

To test this hypothesis, groups of SPF mice were treated with a single dose of ChA or ChB1-Epo2 (40 mg/kg), respectively, or with clindamycin (10 mg/kg) or vancomycin (20 mg/kg) as controls followed by infection with 10^4 spores *C. difficile* VPI10463 on the next day (day 0) (Figure 6D). In line with previous findings, clindamycin-[33] and vancomycin-treated[43] mice suffered from a steep weight loss starting 1 day p.i., demonstrating that both antibiotics disrupt CR and cause susceptibility to CDI (Figure 6E). Remarkably, neither ChA- nor ChB1-Epo2-treatment led to phenotypic disease. Moreover, although clindamycin and vancomycin treatments enabled *C. difficile* colonization, no vegetative cells or spores were detected in chlorotonil-treated mice (Figure 6E). Together, these results demonstrate that, unlike vancomycin and clindamycin, ChA and ChB1-Epo2 exhibit less harmful effects on commensal bacteria that share a nutritional niche with *C. difficile* or produce CR-associated metabolites, thus keeping CR against *C. difficile* intact.

ChA, and to a lesser degree chlorotonil B1-Epo2, inhibits outgrowth of *C. difficile* spores into vegetative cells

Although spores are typically resistant against known antibiotics, the reduction of rCDI by ChA tempted us to hypothesize that ChA affects spore germination or outgrowth into vegetative cells, thereby preventing rCDI. To test this hypothesis, we incubated spores of *C. difficile* (strain VPI10463) with antibiotics for 1 h, followed by plating on agar supplemented with taurocholic acid (TCA) to induce spore germination (Figure 7A). Surprisingly, ChA treatment resulted in inhibition of spore outgrowth and colony formation starting already at 0.1 μg/mL (Figure 7B). Of note, concentrations of 0.4 μg/mL ChA and above completely inhibited colony formation. ChB1-Epo2 was approx. 4- to 8-fold more active against vegetative cells than ChA but was less potent against spores (Figures 1C and 7B). It gradually reduced the number of detectable colonies, leading to an 8-fold reduction at a concentration of 0.1 μg/mL and a 68-fold reduction at a concentration of 0.4 μg/mL, while some colonies were still detected even at the highest concentration (Figure 7B). When spores were plated together with chlorotonils without previous incubation, we observed no changes in CFU count (Figure S6A), indicating that chlorotonils were not simply carried over in the assay. In contrast, vancomycin or metronidazole failed to inhibit spore outgrowth at all tested concentrations (Figure S6B). Fidaxomicin, for which persistence on spores at high concentrations was reported,[44,45] failed in our assays to inhibit colony formation until very high concentrations of 409.6 μg/mL (Figure 7B).

Inhibition of colony formation was also observed after extended cultivation on agar plates up to 72 h (Figure S7C). To exclude the possibility that the plating conditions were responsible for this inhibition, we incubated spores after treatment and washing in liquid media with TCA to induce germination. Similarly, a concentration-dependent effect was observed, with ChA (Figure 7C) exhibiting a stronger effect than ChB1-Epo2(Figure S6D). Spores treated with more than 0.4 μg/mL ChA were subsequently not able to grow in liquid culture within 48 h. After ChB1-Epo2 treatment, *C. difficile* was ultimately able to grow out with up to 6.4 μg/mL initial concentration, a finding that further corroborates distinct activities of the two compounds (Figure 7C).

We next investigated whether chlorotonils are able to inhibit the germination of spores, similar to secondary BAs, and thereby sustain dormancy. Spore germination was characterized by loss of optical density (OD) due to core rehydration[46,47] in the presence of spore germinants and antibiotics. Spores were able to germinate even after ChA or ChB1-Epo2 treatment (6.4 μg/mL). This suggests that chlorotonils inhibit *C. difficile* spore outgrowth rather than germination itself (Figure 7D).

Chlorotonils persist on *C. difficile* spores and prevent lethal infection in mice

Considering that spore incubation with chlorotonils is necessary for inhibition, we hypothesized that, owing to their high hydrophobic character,[31] they persist on *C. difficile* spores. We adapted our inhibition assay to include washing steps with hydrophilic and lipophilic solutions. After repeated washing with PBS, the outgrowth of spores treated with ChA ($p < 0.001$) and ChB1-Epo2 ($p = 0.15$) was still considerably reduced (Figure 7E), albeit at lower efficacy than observed before (Figure 7B). In contrast, washing the spores with 70% ethanol completely negated any inhibition of *C. difficile* spore outgrowth. Washing with 10% ethanol did not decrease inhibition of spore outgrowth, demonstrating that high concentrations of an organic solvent are required to remove ChA from spores. To further validate this finding, we added chlorotonil-treated and washed spores on BHI-agar pre-incubated with *B. subtilis*, which is susceptible to ChA and ChB1-Epo2 (MIC: ChA, 0.4 μg/mL; ChB1-Epo2, 0.2 μg/mL). Strikingly, we observed large *B. subtilis* inhibition zones surrounding spores washed with PBS and 10% ethanol, but not 70% ethanol, thus demonstrating the persistence of chlorotonils on *C. difficile* spores (Figure 7F). Further spore dilutions suggested that ChA and ChB1-Epo2 persist on spores in high concentrations (Figures 7G and S6E).

We next assessed whether ChA is also able to inhibit spore outgrowth *in vivo*. Hence, we pre-treated mice with clindamycin to induce susceptibility (day 1), followed by infection with 10^4 ChA-treated or untreated *C. difficile* VPI10463 spores (Figure 7H). Strikingly, on day 1 and 2 p.i., mice infected with ChA-treated spores exhibit significantly lower body weight loss compared with mice infected with untreated spores, demonstrating a slower and less severe disease progression (Figure 7I). At the end of the experiments, we observed a striking difference in survival rates, with ChA-spore infected mice exhibiting a significantly higher survival rate of 100% in comparison with 33.3% (3/9 mice) in the control group (Figure S6F). Of note, CFU of vegetative cells are significantly decreased in ChA-spore infected mice, across the experiment (day 1, 3, 5, and 7) p.i. (Figure 7J). Furthermore, we did not detect *C. difficile* spores at day 1 p.i. in ChA-spore infected mice, indicating that ChA significantly alters *C. difficile* population dynamics *in vivo*.

In summary, these results demonstrate that chlorotonils, particularly ChA, are able to persist on *C. difficile* spores and thus inhibit outgrowth into vegetative cells even at low physiological concentrations. Furthermore, ChA persisting on *C. difficile* spores prevented lethal infection outcome, making ChA an ideal drug candidate.

DISCUSSION

CDI is in most cases acquired after administration of broad-spectrum antibiotics for an unrelated infection.[48] The unintended

CellPress
OPEN ACCESS

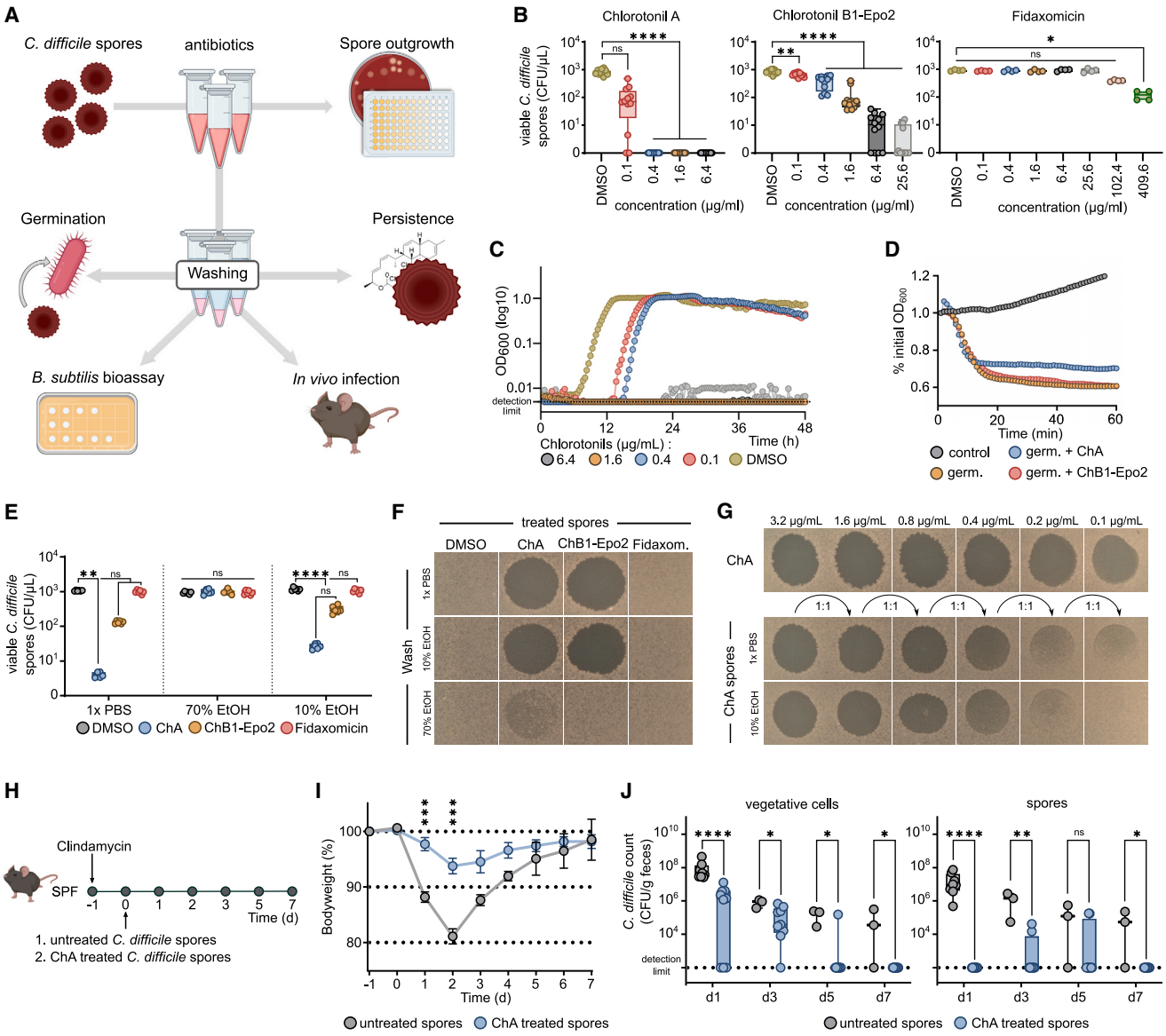

Figure 7. Chlorotonils persist on *C. difficile* spores and inhibit outgrowth into vegetative cells

(A) Experimental setup of extensive spore inhibition assays for (B)–(J).

(B) Concentration-dependent inhibition of *C. difficile* spore outgrowth after incubation with ChA, ChB1-Epo2 and fidaxomicin determined by CFU count on plate. Concentrations above 6.4 µg/mL exceed the aqueous solubility of ChA and were therefore left out.

(C) *C. difficile* spores were treated with decreasing concentrations of ChA, thoroughly washed and incubated in liquid media + 0.1% TCA. Antibiotics were absent from the media used for outgrowth. Growth was measured over a period of 48 h. Dotted line represents detection limit.

(D) Germination assay determined by loss of OD_{600} over a time course of 1 h in the presence of 6.4 µg/mL ChA or ChB1-Epo2.

(E) Inhibition of spore outgrowth by 6.4 µg/mL ChA or ChB1-Epo2 treatment, followed by extensive washing with 1× PBS, 70% EtOH, and 10% EtOH, determined by CFU on plate.

(F and G) Persistence of ChA and ChB1-Epo2 was validated by adding (F) concentrated or (G) diluted spores from (E) on brain heart infusion (BHI)-agar pre-incubated with *B. subtilis*. Bioassay plates were grown aerobically for 24 h at 37°C.

(H) SPF (n = 9/group) mice were pre-treated with clindamycin (10 mg/kg) (day −1) and infected with 10^4 ChA-treated or control-treated and PBS washed *C. difficile* spores (day 0).

(I) Average daily weight of mice infected with either control-treated or ChA-treated spores.

(J) Fecal burden of *C. difficile* vegetative cells and spores at different infection time points. Dotted line represents detection limit. p values in (B) and (E) represent Kruskall-Wallis one-way ANOVA between samples and DMSO control. p values in (I) and (J) Mann-Whitney non-parametric rank comparison, between treatment groups at specific infection time point. Error bars represent ± SEM. (*p < 0.05, **p < 0.01, ***p < 0.001, ****p < 0.0001).

See also Figure S6.

damage of the intestinal microbiota creates a luminal environment permissive to *C. difficile* spore germination, vegetative growth, and ultimately intestinal damage. CDI remains a major healthcare problem, since the antibiotics currently used to treat CDI, i.e., vancomycin and metronidazole, sustain the functionally impaired microbiota. In combination with the persistence of endospores, this results in high rates of recurrent infections occurring in approximately 20% of all patients.[49,50] A newer and more costly treatment is fidaxomicin, which is efficient against *C. difficile* without the high incidence of recurrent infections of many clinical isolates. However, treatment efficacy of rCDI did not differ between fidaxomicin and vancomycin for infections with RT 027, a hypervirulent variant linked to several *C. difficile* epidemics.[22,51] Consequently, the need for *C. difficile* targeting antibiotics with little impact on CR against *C. difficile* is growing to ensure proper treatment and reduce the risk of recurrent infections or other adverse effects caused by a less intact microbiota.

Strikingly, chlorotonils, particularly ChA, fulfill these criteria. First, both ChA and ChB1-Epo2 have activity against the vegetative cells of *C. difficile* strains, including strains resistant against commonly used antibiotics. Second, ChA,[31] similarly to vancomycin,[52] exhibits a low systemic bioavailability after oral application, being predominantly present in the intestine, a property desired for treating CDI. Interestingly, ChA has a longer transit time than vancomycin, which could eventually be beneficial for clinical dosing schemes. Third, ChA preserves microbiota function *in vivo*. Notably, although treatment of mice with vancomycin breaks CR against *C. difficile*, chlorotonils sustained CR *in vivo*. This was associated with maintenance of intestinal BA metabolism for both chlorotonils, and for ChA with homeostatic levels of SCFAs, as well as Stickland fermentation substrates and products. Fourth, ChA, and to a lesser degree ChB1-Epo2, are able to inhibit spore outgrowth into vegetative cells at biologically relevant concentrations. Altogether, our data suggest that ChA inhibits (r)CDI by its direct activity against vegetative cells, its persistence on spores of *C. difficile*, and by allowing the faster regeneration of the intestinal microbiota.

Particularly, the persistence of ChA on *C. difficile* spores and its potential consequences for preventing rCDI are of high interest. Although ChA did not induce direct spore lysis or destruction of *C. difficile* spores similar to chemical-disinfectant-type molecules,[24] the inhibition of spore outgrowth by chlorotonils at concentrations similar to MIC values of vegetative cells and in the range of biologically relevant concentrations was unexpected. Notably, persistence of antibiotics on *C. difficile* spores was observed before for fidaxomicin at concentrations far exceeding the MIC for vegetative cells, i.e., >1,000-fold the MIC for its spore-binding inhibitory activity.[44] Interestingly, the inhibitory activity of chlorotonils was removed only by a series of washing steps with organic solvents, which indicates that hydrophobic antibiotics, such as chlorotonils, persist in the hydrophobic spore coats, as demonstrated by the inhibition of ChA-sensitive bacteria after co-incubation with ChA-loaded and washed spores. Moreover, ChA-treated spores were strongly impaired in their ability to germinate *in vivo* and cause CDI, highlighting the potency of this class of molecules against different forms of *C. difficile*. Additional studies will be required to clarify the persistence of ChA on spores of other spore-forming commensal bacteria that contribute important functions to CR, as differences in the species-specific composition of spores could impact the ability of ChA to be retained in the spore.

Although we described in this study the antimicrobial properties of chlorotonils in diverse model systems, the exact mode-of-action and molecular target of this natural product class remain unknown. Specifically, whether ChA truly acts bactericidal or rather bacteriostatic remains to be conclusively demonstrated, particularly in light of a recent study that revealed that whether antibiotics act bactericidal or bacteriostatic may depend on the species.[53] Integrated transcriptome, proteome, and metallome analyses of chlorotonil treatment uncovered substantial reprogramming of the energy, AA, and carbohydrate metabolism even at sublethal concentrations, and supported that ChB1-Epo2 interferes with main cellular processes of *C. difficile*, contributing to gut colonization. Notably, metal homeostasis can severely affect *C. difficile's* competitive fitness *in vitro* and *in vivo*[54] and its modulation by ChB1-Epo2 may contribute to the therapeutic effect of chlorotonils. The differences observed between ChA and ChB1-Epo2 in their activity on vegetative cells and in their binding to spores may be explained by their distinct physicochemical properties, specifically their hydrophobicity, and by targeting proteins with different abundances during vegetative growth and outgrowth from spores. Importantly, the identification of the target will provide further insight into why *C. difficile* is particularly sensitive to the chlorotonils *in vivo* compared with other commensal bacteria, especially why some Gram-positive families were reduced and others enriched or unchanged. For instance, ChA treatment of piglets resulted in specific detrimental effects on the genera *Clostridium* and *Terrisporobacter*. This may be the result of a particularly strong affinity between the target in *C. difficile* and ChA and ChB1-Epo2, respectively, compared with the target in other commensal bacteria or a key function of the target in *C. difficile* resulting in competitive disadvantages against unaffected or less affected commensal bacteria, even at sub-MIC concentrations.

In summary, our findings describe an underexplored antibacterial compound class with mild and specific effects on the murine and porcine microbiota. In particular, ChA is a promising candidate for the treatment of CDI due to its capacity to both antagonize an established CDI and prevent relapses, as observed after vancomycin treatment. Beneficial commensals, which rely on distinct metabolic pathways, are able to resist chlorotonil treatment or rapidly recover growth, thus re-establishing CR. Consequently, the pathogen will more easily be replaced from its metabolic niche by commensal bacteria within the gut. Future investigations will be required to identify the molecular targets and processes affected by this class of natural products. We conclude that compounds such as the chlorotonils, which maintain key functionalities of the microbiota critical for the defense against infections and mutualistic interactions with the host, will open broad possibilities for therapeutic interventions.

STAR★METHODS

Detailed methods are provided in the online version of this paper and include the following:

- KEY RESOURCES TABLE
- RESOURCE AVAILABILITY

SUPPLEMENTAL INFORMATION

Supplemental information can be found online at https://doi.org/10.1016/j.chom.2023.04.003.

ACKNOWLEDGMENTS

We thank the staff of the animal facilities at HZI and FLI. Ina Schleicher, Vera Junker, Gesa Martens, and Anika Wasner are acknowledged for technical assistance. We thank Klaus Neuhaus and Caroline Ziegler from the TUM Core Facility Microbiome for NGS. We are grateful to Wiep Klaas Smits for providing *C. difficile* strain IB136 and Karl Gademann for providing fidaxomicin. We thank Anastasia Andreas for the help in the extraction of the piglet feces and Franziska Faber and Caroline Taouk for reading the manuscript. This study was supported by a grant from the BMBF (Federal Ministry of Education and Research of Germany) within the frame of InfectControl 2020 to KR and TMF (FKZ 03ZZ0823A/B), and by grants of the Deutsche Forschungsgemeinschaft under Germany's Excellence Strategy—EXC 2155 "RESIST"—project ID 390874280. Improvement and assessments of the compounds were supported by a grant from the BMBF to R.M. during the ChloroClinaria Project (16GW0204K). Parts of the figures were created using BioRender.com and "Inkscape".

AUTHOR CONTRIBUTIONS

A.B., M.B., and S.W. designed, conducted, and analyzed experiments and wrote the manuscript; W.H. synthesized ChB1-Epo2 and conducted and analyzed experiments; M.M., F.D., M.N.-S., L.-S.P., J.B., A.M.K., and D.Z. conducted and analyzed experiments; T.R.L. analyzed experiments and supported with bioinformatic analysis; U.N. provided essential reagents and analyzed experiments; S.B. optimized and M.N.-S. coordinated production of ChA; R.J. optimized isolation and analysis of ChA; S.S. designed and analyzed experiments; K.R. and R.M. designed the study; J.H. designed and coordinated the study; T.M.F. and T.S. designed and coordinated the study, analyzed data, and wrote the manuscript.

DECLARATION OF INTERESTS

S.B., R.J., J.H., and R.M. are listed as inventors of a patent of the use of chlorotonils as antimicrobial agent (WO/2019/092030). This has not interfered with the design of the study and the interpretation of results.

INCLUSION AND DIVERSITY

We support inclusive, diverse, and equitable conduct of research.

Received: April 27, 2022
Revised: February 24, 2023
Accepted: April 3, 2023
Published: April 24, 2023

REFERENCES

1. Knight, D.R., and Riley, T.V. (2019). Genomic delineation of zoonotic origins of Clostridium difficile. Front. Public Heal. *7*, 164. https://doi.org/10.3389/fpubh.2019.00164.
2. Balsells, E., Shi, T., Leese, C., Lyell, I., Burrows, J., Wiuff, C., Campbell, H., Kyaw, M.H., and Nair, H. (2019). Global burden of Clostridium difficile infections: A systematic review and meta-analysis. J. Glob. Health *9*, 010407. https://doi.org/10.7189/jogh.09.010407.
3. Finn, E., Andersson, F.L., and Madin-Warburton, M. (2021). Burden of Clostridioides difficile infection (CDI) - a systematic review of the epidemiology of primary and recurrent CDI. BMC Infect. Dis. *21*, 456. https://doi.org/10.1186/s12879-021-06147-y.
4. Sholeh, M., Krutova, M., Forouzesh, M., Mironov, S., Sadeghifard, N., Molaeipour, L., Maleki, A., and Kouhsari, E. (2020). Antimicrobial resistance in Clostridioides (Clostridium) difficile derived from humans: a systematic review and meta-analysis. Antimicrob. Resist. Infect. Control *9*, 158. https://doi.org/10.1186/s13756-020-00815-5.
5. van Werkhoven, C.H., Ducher, A., Berkell, M., Mysara, M., Lammens, C., Torre-Cisneros, J., Rodríguez-Baño, J., Herghea, D., Cornely, O.A., Biehl, L.M., et al. (2021). Incidence and predictive biomarkers of Clostridioides difficile infection in hospitalized patients receiving broad-spectrum antibiotics. Nat. Commun. *12*, 2240. https://doi.org/10.1038/s41467-021-22269-y.
6. Theriot, C.M., Koenigsknecht, M.J., Carlson, P.E., Hatton, G.E., Nelson, A.M., Li, B., Huffnagle, G.B., Z Li, J.Z., and Young, V.B. (2014). Antibiotic-induced shifts in the mouse gut microbiome and metabolome increase susceptibility to Clostridium difficile infection. Nat. Commun. *5*, 3114. https://doi.org/10.1038/ncomms4114.
7. Britton, R.A., and Young, V.B. (2014). Role of the intestinal microbiota in resistance to colonization by Clostridium difficile. Gastroenterology *146*, 1547–1553. https://doi.org/10.1053/j.gastro.2014.01.059.

8. Martinez-Gili, L., McDonald, J.A.K., Liu, Z., Kao, D., Allegretti, J.R., Monaghan, T.M., Barker, G.F., Miguéns Blanco, J., Williams, H.R.T., Holmes, E., et al. (2020). Understanding the mechanisms of efficacy of fecal microbiota transplant in treating recurrent *Clostridioides difficile* infection and beyond: the contribution of gut microbial-derived metabolites. Gut Microbes *12*, 1810531. https://doi.org/10.1080/19490976.2020.1810531.

9. Lesniak, N.A., Schubert, A.M., Sinani, H., and Schloss, P.D. (2021). Clearance of Clostridioides difficile colonization is associated with antibiotic-specific bacterial changes. mSphere *6*. e01238-e01220. https://doi.org/10.1128/mSphere.01238-20.

10. Cornely, O.A., Miller, M.A., Louie, T.J., Crook, D.W., and Gorbach, S.L. (2012). Treatment of first recurrence of clostridium difficile infection: fidaxomicin versus vancomycin. Clin. Infect. Dis. *55*, S154–S161. https://doi.org/10.1093/cid/cis462.

11. Isaac, S., Scher, J.U., Djukovic, A., Jiménez, N., Littman, D.R., Abramson, S.B., Pamer, E.G., and Ubeda, C. (2017). Short- and long-term effects of oral vancomycin on the human intestinal microbiota. J. Antimicrob. Chemother. *72*, 128–136. https://doi.org/10.1093/JAC/DKW383.

12. Warren, C.A., van Opstal, E.J., Riggins, M.S., Li, Y., Moore, J.H., Kolling, G.L., Guerrant, R.L., and Hoffman, P.S. (2013). Vancomycin treatment's association with delayed intestinal tissue injury, clostridial overgrowth, and recurrence of Clostridium difficile infection in mice. Antimicrob. Agents Chemother. *57*, 689–696. https://doi.org/10.1128/AAC.00877-12.

13. Reed, A.D., and Theriot, C.M. (2021). Contribution of inhibitory metabolites and competition for nutrients to colonization resistance against Clostridioides difficile by commensal clostridium. Microorganisms *9*, 1–14. https://doi.org/10.3390/microorganisms9020371.

14. Reed, A.D., Nethery, M.A., Stewart, A., Barrangou, R., and Theriot, C.M. (2020). Strain-dependent inhibition of Clostridioides difficile by commensal clostridia carrying the bile acid-inducible (bai) operon. J. Bacteriol. *202*. e00039-e00020. https://doi.org/10.1128/JB.00039-20.

15. Buffie, C.G., Bucci, V., Stein, R.R., McKenney, P.T., Ling, L., Gobourne, A., Liu, H., Kinnebrew, M., Viale, A., et al. (2015). Precision microbiome reconstitution restores bile acid mediated resistance to Clostridium difficile. Nature *517*, 205–208. https://doi.org/10.1038/nature13828.

16. Battaglioli, E.J., Hale, V.L., Chen, J., Jeraldo, P., Ruiz-Mojica, C., Schmidt, B.A., Rekdal, V.M., Till, L.M., Huq, L., Smits, S.A., et al. (2018). Clostridioides difficile uses amino acids associated with gut microbial dysbiosis in a subset of patients with diarrhea. Sci. Transl. Med. *10*, 139–148. https://doi.org/10.1126/scitranslmed.aam7019.

17. Girinathan, B.P., DiBenedetto, N., Worley, J.N., Peltier, J., Arrieta-Ortiz, M.L., Immanuel, S.R.C., Lavin, R., Delaney, M.L., Cummins, C.K., Hoffman, M., et al. (2021). In vivo commensal control of Clostridioides difficile virulence. Cell Host Microbe *29*, 1693–1708.e7. https://doi.org/10.1016/J.CHOM.2021.09.007.

18. Janoir, C., Denève, C., Bouttier, S., Barbut, F., Hoys, S., Caleechum, L., Chapetón-Montes, D., Pereira, F.C., Henriques, A.O., Collignon, A., et al. (2013). Adaptive strategies and pathogenesis of Clostridium difficile from in vivo transcriptomics. Infect. Immun. *81*, 3757–3769. https://doi.org/10.1128/IAI.00515-13.

19. Fletcher, J.R., Pike, C.M., Parsons, R.J., Rivera, A.J., Foley, M.H., McLaren, M.R., Montgomery, S.A., and Theriot, C.M. (2021). Clostridioides difficile exploits toxin-mediated inflammation to alter the host nutritional landscape and exclude competitors from the gut microbiota. Nat. Commun. *12*, 462. https://doi.org/10.1038/s41467-020-20746-4.

20. Poquet, I., Saujet, L., Canette, A., Monot, M., Mihajlovic, J., Ghigo, J.M., Soutourina, O., Briandet, R., Martin-Verstraete, I., and Dupuy, B. (2018). Clostridium difficile biofilm: remodeling metabolism and cell surface to build a sparse and heterogeneously aggregated architecture. Front. Microbiol. *9*, 2084. https://doi.org/10.3389/fmicb.2018.02084.

21. Chaar, A., and Feuerstadt, P. (2021). Evolution of clinical guidelines for antimicrobial management of Clostridioides difficile infection. Ther. Adv. Gastroenterol. *14*, 17562848211011953. https://doi.org/10.1177/17562848211011953.

22. Louie, T.J., Miller, M.A., Mullane, K.M., Weiss, K., Lentnek, A., Golan, Y., Gorbach, S., Sears, P., and Shue, Y.K.; OPT-80-003 Clinical Study Group (2011). Fidaxomicin versus vancomycin for Clostridium difficile Infection. N. Engl. J. Med. *364*, 422–431. https://doi.org/10.1056/NEJMoa0910812.

23. Schwanbeck, J., Riedel, T., Laukien, F., Schober, I., Oehmig, I., Zimmermann, O., Overmann, J., Groß, U., Zautner, A.E., and Bohne, W. (2019). Characterization of a clinical Clostridioides difficile isolate with markedly reduced fidaxomicin susceptibility and a V1143D mutation in rpoB. J. Antimicrob. Chemother. *74*, 6–10. https://doi.org/10.1093/jac/dky375.

24. Russell, A.D. (1990). Bacterial spores and chemical sporicidal agents. Clin. Microbiol. Rev. *3*, 99–119. https://doi.org/10.1128/CMR.3.2.99.

25. Paredes-Sabja, D., Shen, A., and Sorg, J.A. (2014). Clostridium difficile spore biology: sporulation, germination, and spore structural proteins. Trends Microbiol. *22*, 406–416. https://doi.org/10.1016/j.tim.2014.04.003.

26. Baloh, M., and Sorg, J.A. (2022). Clostridioides difficile spore germination: initiation to DPA release. Curr. Opin. Microbiol. *65*, 101–107. https://doi.org/10.1016/j.mib.2021.11.001.

27. Miethke, M., Pieroni, M., Weber, T., Brönstrup, M., Hammann, P., Halby, L., Arimondo, P.B., Glaser, P., Aigle, B., Bode, H.B., et al. (2021). Towards the sustainable discovery and development of new antibiotics. Nat. Rev. Chem. *5*, 726–749. https://doi.org/10.1038/s41570-021-00313-1.

28. Gerth, K., Steinmetz, H., Höfle, G., and Jansen, R. (2008). Chlorotonil A, a macrolide with a unique gem-dichloro-1,3-dione functionality from Sorangium cellulosum, So CE1525. Angew. Chem. Int. Ed. Engl. *47*, 600–602. https://doi.org/10.1002/anie.200703993.

29. Jungmann, K., Jansen, R., Gerth, K., Huch, V., Krug, D., Fenical, W., and Müller, R. (2015). Two of a kind—the biosynthetic pathways of chlorotonil and Anthracimycin. ACS Chem. Biol. *10*, 2480–2490. https://doi.org/10.1021/ACSCHEMBIO.5B00523.

30. Held, J., Gebru, T., Kalesse, M., Jansen, R., Gerth, K., Müller, R., and Mordmüller, B. (2014). Antimalarial activity of the myxobacterial macrolide chlorotonil A. Antimicrob. Agents Chemother. *58*, 6378–6384. https://doi.org/10.1128/AAC.03326-14.

31. Hofer, W., Oueis, E., Fayad, A.A., Deschner, F., Andreas, A., de Carvalho, L.P., Hüttel, S., Bernecker, S., Pätzold, L., Morgenstern, B., et al. (2022). Regio- and stereoselective epoxidation and acidic epoxide opening of antibacterial and antiplasmodial chlorotonils yield highly potent derivatives. Angew. Chem. Int. Ed. Engl. *61*, e202202816. https://doi.org/10.1002/anie.202202816.

32. Lozupone, C., and Knight, R. (2005). UniFrac: a new phylogenetic method for comparing microbial communities. Appl. Environ. Microbiol. *71*, 8228–8235. https://doi.org/10.1128/AEM.71.12.8228-8235.2005.

33. Xiao, L., Estellé, J., Kiilerich, P., Ramayo-Caldas, Y., Xia, Z., Feng, Q., Liang, S., Pedersen, A.Ø., Kjeldsen, N.J., Liu, C., et al. (2016). A reference gene catalogue of the pig gut microbiome. Nat. Microbiol. *1*, 16161. https://doi.org/10.1038/nmicrobiol.2016.161.

34. Sorbara, M.T., and Pamer, E.G. (2019). Interbacterial mechanisms of colonization resistance and the strategies pathogens use to overcome them. Mucosal Immunol. *12*, 1–9. https://doi.org/10.1038/s41385-018-0053-0.

35. Gregory, A.L., Pensinger, D.A., and Hryckowian, A.J. (2021). A short chain fatty acid-centric view of Clostridioides difficile pathogenesis. PLoS Pathog. *17*, e1009959. https://doi.org/10.1371/journal.ppat.1009959.

36. Aguirre, A.M., Yalcinkaya, N., Wu, Q., Swennes, A., Tessier, M.E., Roberts, P., Miyajima, F., Savidge, T., and Sorg, J.A. (2021). Bile acid-independent protection against Clostridioides difficile infection. PLoS Pathog. *17*, e1010015. https://doi.org/10.1371/journal.ppat.1010015.

37. Bouillaut, L., Self, W.T., and Sonenshein, A.L. (2013). Proline-dependent regulation of Clostridium difficile stickland metabolism. J. Bacteriol. *195*, 844–854. https://doi.org/10.1128/JB.01492-12.

38. Reed, A.D., Fletcher, J.R., Huang, Y.Y., Thanissery, R., Rivera, A.J., Parsons, R.J., Stewart, A.K., Kountz, D.J., Shen, A., Balskus, E.P., et al. (2022). The Stickland Reaction Precursor trans -4-hydroxy- l -proline

Differentially Impacts the Metabolism of Clostridioides difficile and Commensal Clostridia. mSphere *7*, e0092621. https://doi.org/10.1128/msphere.00926-21.

39. Erikstrup, L.T., Aarup, M., Hagemann-Madsen, R., Dagnaes-Hansen, F., Kristensen, B., Olsen, K.E.P., and Fuursted, K. (2015). Treatment of Clostridium difficile infection in mice with vancomycin alone is as effective as treatment with vancomycin and metronidazole in combination. BMJ Open Gastroenterol. *2*, e000038. https://doi.org/10.1136/BMJGAST-2015-000038.
40. Chilton, C.H., Crowther, G.S., Ashwin, H., Longshaw, C.M., and Wilcox, M.H. (2016). Association of fidaxomicin with C. difficile spores: effects of persistence on subsequent spore recovery, outgrowth and toxin production. PLoS One *11*, e0161200. https://doi.org/10.1371/journal.pone.0161200.
41. Chilton, C.H., Ashwin, H., and Crowther, G.S. (2014). P0799 Persistence and removal of fidaxomicin from C. difficile spores, and effects on recovery. European Conference on Clinical Microbiology and Infectious Disease (ECCMID), 1–2.
42. Kochan, T.J., Somers, M.J., Kaiser, A.M., Shoshiev, M.S., Hagan, A.K., Hastie, J.L., Giordano, N.P., Smith, A.D., Schubert, A.M., Carlson, P.E., et al. (2017). Intestinal calcium and bile salts facilitate germination of Clostridium difficile spores. PLoS Pathog. *13*, e1006443. https://doi.org/10.1371/journal.ppat.1006443.
43. Francis, M.B., Allen, C.A., and Sorg, J.A. (2015). Spore cortex hydrolysis precedes dipicolinic acid release during Clostridium difficile spore germination. J. Bacteriol. *197*, 2276–2283. https://doi.org/10.1128/JB.02575-14.
44. Dharbhamulla, N., Abdelhady, A., Domadia, M., Patel, S., Gaughan, J., and Roy, S. (2019). Risk factors associated with recurrent Clostridium difficile infection. J. Clin. Med. Res. *11*, 1–6. https://doi.org/10.14740/jocmr3531w.
45. Mullish, B.H., and Williams, H.R.T. (2018). Clostridium diffi cile infection and antibiotic-associated diarrhoea. Clin. Med. (Lond) *18*, 237–241. https://doi.org/10.7861/clinmedicine.18-3-237.
46. Hopkins, R.J., and Wilson, R.B. (2018). Treatment of recurrent Clostridium difficile colitis: a narrative review. Gastroenterol. Rep. *6*, 21–28. https://doi.org/10.1093/gastro/gox041.
47. Yakob, L., Riley, T.V., Paterson, D.L., Marquess, J., Magalhaes, R.J.S., Furuya-Kanamori, L., and Clements, A.C.A. (2015). Mechanisms of hypervirulent Clostridium difficile ribotype 027 displacement of endemic strains: an epidemiological model. Sci. Rep. *5*, 12666. https://doi.org/10.1038/srep12666.
48. Patel, S., Preuss, C.V., and Bernice, F. (2022). Vancomycin – StatPearls – NCBI bookshelf. StatPearls. https://www.ncbi.nlm.nih.gov/books/NBK459263/.
49. Maier, L., Goemans, C.V., Wirbel, J., Kuhn, M., Eberl, C., Pruteanu, M., Müller, P., Garcia-Santamarina, S., Cacace, E., Zhang, B., et al. (2021). Unravelling the collateral damage of antibiotics on gut bacteria. Nature *599*, 120–124. https://doi.org/10.1038/s41586-021-03986-2.
50. Lopez, C.A., Beavers, W.N., Weiss, A., Knippel, R.J., Zackular, J.P., Chazin, W., and Skaar, E.P. (2019). The immune protein calprotectin impacts Clostridioides difficile metabolism through zinc limitation. mBio *10*, 1–19.
51. Neumann-Schaal, M., Hofmann, J.D., Will, S.E., and Schomburg, D. (2015). Time-resolved amino acid uptake of Clostridium difficile 630Δerm and concomitant fermentation product and toxin formation. BMC Microbiol. *15*, 281. https://doi.org/10.1186/s12866-015-0614-2.
52. Edwards, A.N., Suárez, J.M., and McBride, S.M. (2013). Culturing and maintaining Clostridium difficile in an anaerobic environment. J. Vis. Exp. *79*, e50787. https://doi.org/10.3791/50787.
53. Theriot, C.M., Bowman, A.A., and Young, B. (2016). Antibiotic-induced alterations of the gut difficile Spore germination and outgrowth in the large intestine. mSphere *1*, 1–16. https://doi.org/10.1128/mSphere.00045-15.Editor.
54. Su, W.J., Waechter, M.J., Bourlioux, P., Dolegeal, M., Fourniat, J., and Mahuzier, G. (1987). Role of volatile fatty acids in colonization resistance to Clostridium difficile in gnotobiotic mice. Infect. Immun. *55*, 1686–1691. https://doi.org/10.1128/iai.55.7.1686-1691.1987.
55. Caporaso, J.G., Lauber, C.L., Walters, W.A., Berg-Lyons, D., Lozupone, C.A., Turnbaugh, P.J., Fierer, N., and Knight, R. (2011). Global patterns of 16S rRNA diversity at a depth of millions of sequences per sample. Proc. Natl. Acad. Sci. USA *108*, 4516–4522. https://doi.org/10.1073/pnas.1000080107.
56. Price, M.N., Dehal, P.S., and Arkin, A.P. (2010). FastTree 2--approximately maximum-likelihood trees for large alignments. PLoS One *5*, e9490. https://doi.org/10.1371/journal.pone.0009490.
57. Wang, Q., Garrity, G.M., Tiedje, J.M., and Cole, J.R. (2007). Naive Bayesian classifier for rapid assignment of rRNA sequences into the new bacterial taxonomy. Appl. Environ. Microbiol. *73*, 5261–5267. https://doi.org/10.1128/AEM.00062-07.
58. Edgar, R.C. (2010). Search and clustering orders of magnitude faster than BLAST. Bioinformatics *26*, 2460–2461. https://doi.org/10.1093/bioinformatics/btq461.
59. McMurdie, P.J., and Holmes, S. (2013). phyloseq: an R package for reproducible interactive analysis and graphics of microbiome census data. PLoS One *8*, e61217. https://doi.org/10.1371/journal.pone.0061217.
60. Hofmann, J.D., Otto, A., Berges, M., Biedendieck, R., Michel, A.M., Becher, D., Jahn, D., and Neumann-Schaal, M. (2018). Metabolic reprogramming of Clostridioides difficile during the stationary phase with the induction of toxin production. Front. Microbiol. *9*, 1970. https://doi.org/10.3389/fmicb.2018.01970.
61. Will, S.E., Henke, P., Boedeker, C., Huang, S., Brinkmann, H., Rohde, M., Jarek, M., Friedl, T., Seufert, S., Schumacher, M., et al. (2019). Day and night: metabolic profiles and evolutionary relationships of six axenic non-marine cyanobacteria. Genome Biol. Evol. *11*, 270–294. https://doi.org/10.1093/gbe/evy275.
62. Hu, C., Beyda, N.D., and Garey, K.W. (2022). A vancomycin HPLC assay for use in gut microbiome research. Microbiol. Spectr. *10*, e0168821. https://doi.org/10.1128/spectrum.01688-21.
63. Caporaso, J.G., Kuczynski, J., Stombaugh, J., Bittinger, K., Bushman, F.D., Costello, E.K., Fierer, N., Peña, A.G., Goodrich, J.K., Gordon, J.I., et al. (2010). correspondence QIIME allows analysis of high- throughput community sequencing data Intensity normalization improves color calling in SOLiD sequencing. Nat. Publ. Gr. *7*, 335–336. https://doi.org/10.1038/nmeth0510-335.
64. Lagkouvardos, I., Kläring, K., Heinzmann, S.S., Platz, S., Scholz, B., Engel, K.-H., Schmitt-Kopplin, P., Haller, D., Rohn, S., Skurk, T., et al. (2015). Gut metabolites and bacterial community networks during a pilot intervention study with flaxseeds in healthy adult men. Mol. Nutr. Food Res. *59*, 1614–1628. https://doi.org/10.1002/mnfr.201500125.
65. Lagkouvardos, I., Joseph, D., Kapfhammer, M., Giritli, S., Horn, M., Haller, D., and Clavel, T. (2016). IMNGS: A comprehensive open resource of processed 16S rRNA microbial profiles for ecology and diversity studies. Sci. Rep. *6*, 33721. https://doi.org/10.1038/srep33721.
66. Edgar, R.C., Haas, B.J., Clemente, J.C., Quince, C., and Knight, R. (2011). UCHIME improves sensitivity and speed of chimera detection. Bioinformatics *27*, 2194–2200. https://doi.org/10.1093/bioinformatics/btr381.
67. Pruesse, E., Peplies, J., and Glöckner, F.O. (2012). SINA: accurate high-throughput multiple sequence alignment of ribosomal RNA genes. Bioinformatics *28*, 1823–1829. https://doi.org/10.1093/bioinformatics/bts252.
68. Lagkouvardos, I., Fischer, S., Kumar, N., and Clavel, T. (2017). Rhea: A transparent and modular R pipeline for microbial profiling based on 16S rRNA gene amplicons. PeerJ *2017*, e2836. https://doi.org/10.7717/PEERJ.2836/SUPP-2.
69. Chen, J., Bittinger, K., Charlson, E.S., Hoffmann, C., Lewis, J., Wu, G.D., Collman, R.G., Bushman, F.D., and Li, H. (2012). Associating microbiome composition with environmental covariates using generalized UniFrac distances. Bioinformatics *28*, 2106–2113. https://doi.org/10.1093/bioinformatics/bts342.
70. Jost, L. (2007). Partitioning diversity into independent alpha beta concepts. Ecology *88*, 2427–2439.

71. Goecks, J., Nekrutenko, A., and Taylor, J.; Galaxy Team (2010). Galaxy: a comprehensive approach for supporting accessible, reproducible, and transparent computational research in the life sciences. Genome Biol. *11*, R86. https://doi.org/10.1186/gb-2010-11-8-r86.

72. Graf, A.C., Leonard, A., Schäuble, M., Rieckmann, L.M., Hoyer, J., Maass, S., Lalk, M., Becher, D., Pané-Farré, J., and Riedel, K. (2019). Virulence factors produced by *Staphylococcus aureus* biofilms have a moonlighting function contributing to biofilm integrity. Mol. Cell. Proteomics *18*, 1036–1053. https://doi.org/10.1074/mcp.RA118.001120.

73. Mücke, P.-A., Maaß, S., Kohler, T.P., Hammerschmidt, S., and Becher, D. (2020). Proteomic adaptation of Streptococcus pneumoniae to the human antimicrobial peptide LL-37. Microorganisms *8*, 413. https://doi.org/10.3390/microorganisms8030413.

74. Tyanova, S., Temu, T., and Cox, J. (2016). The MaxQuant computational platform for mass spectrometry-based shotgun proteomics. Nat. Protoc. *11*, 2301–2319. https://doi.org/10.1038/nprot.2016.136.

75. Zhu, Y., Orre, L.M., Zhou Tran, Y.Z., Mermelekas, G., Johansson, H.J., Malyutina, A., Anders, S., and Lehtiö, J. (2020). DEqMS: A method for accurate variance estimation in differential protein expression analysis. Mol. Cell. Proteomics *19*, 1047–1057. https://doi.org/10.1074/mcp.TIR119.001646.

76. Kolde, R. (2019). pheatmap: Pretty Heatmpas. R package version 1.0.12. https://cran.r-project.org/web/packages/pheatmap/index.html.

77. Wojdyr, M. (2010). Fityk: a general-purpose peak fitting program. J. Appl. Crystallogr. *43*, 1126–1128. https://doi.org/10.1107/S0021889810030499.

78. Kassambara, A. (2021). rstatix: pipe-Friendly Framework for Basic Statistical Tests version 0.7.0. https://rdrr.io/github/kassambara/rstatix/.

79. Wickham, H. (2016). ggplot2. Elegant Graphics for Data Analysis, Second Edition (Springer). https://doi.org/10.1007/978-0-387-98141-3.

STAR★METHODS

KEY RESOURCES TABLE

REAGENT or RESOURCE	SOURCE	IDENTIFIER
Bacterial and virus strains		
C. difficile 630	DSMZ	DSM 27543
C. difficile VPI10463	ATCC	ATCC43255
C. difficile 1780	DSMZ	DSM 1296
C. difficile R20291	DSMZ	DSM 27147
C. difficile CD-10-00484 (vancomycin resilient)	PMID 26444881	N/A
C. difficile CD-22-00115 (Metronidazole resistant)	PMID 32001686	N/A
C. difficile CD-22-00001 (Fidaxomicin resistant)	Schwanbeck et al.[23]	N/A
C. difficile CD-15-00638 (vancomycin resilient)	PMID 32726198	N/A
Chemicals, peptides, and recombinant proteins		
Chlorotonil A, B1-Epo2	Helmholtz Institute for Pharmaceutical Research Saarland	N/A
Menadione crystalline (vitamin K)	Sigma-Aldrich	Cat# M5625
Brain Heart Infusion	OXOID	Cat#CM1135B
DMSO	Carl Roth	Cat#A994.2
Vancomycin HCl	Carl Roth	Cat# 0242.3
Metronidazole	Sigma	Cat# 443-48-1
Fidaxomicin	MedChemExpress	Cat# HY-17580
Ethanol	J. T. Baker	Cat# 64-17-5
Clindamycin HCl	Sigma	Cat# 21462-39-5
$CaCl_2 \times 2H_2O$	Merck	N/A
Glycine	Carl Roth	Cat# 0079.1
Triz-Base	Sigma	Cat# 741883
TCA sodium salt	Carl Roth	Cat# 8149.2
L-Cysteine	L-Cysteine	Cat#1693.1
Soy oil	Caelo	Cat#8001-22-7
Critical commercial assays		
Mouse lipocalin-2/NGAL DuoSet ELISA	R&D Systems	Cat#DY1857
Separate detection of C. difficile toxins A and B	tgcBIOMICS	Cat#TGC-E002-1
ZymoBIOMICS 96 MagBead DNA Kit	Zymo Research	Cat#D4302
Deposited data		
16S rRNA gene sequencing of mice	This study	PRJNA809685
16S rRNA gene sequencing of piglets	This study	PRJNA800240
RNA sequencing data	This study	PRJNA949940
Mass spectrometry proteomics data	This study	PXD029243
Experimental models: Organisms/strains		
WT C57BL/6N 6-30 weeks, housed under enhanced specific pathogen free conditions at the animal facility of the Helmholtz Institute for Infection research, Germany	Janvier Labs	N/A
Germ-free WT C57BL/6NTac mice 16 weeks, raised in gnotobiotic isolaters at the germ-free facility of the Helmholtz Institute for Infection research, Germany	Raised in house	N/A
Piglets 4 weeks, housed at the the animal facility of the Friedrich-Loeffler-Institute, Germany	Mörsdorfer Agrar GmbH	N/A

(*Continued on next page*)

Continued

REAGENT or RESOURCE	SOURCE	IDENTIFIER
Oligonucleotides		
Primers for 16 S sequencing 16S_V4Seq_515F: 5'AATGA TACGGCGACCACCGAGAT CTACACTATGGTAATTGTG TGCCAGCMGCCGCGGTAA 16S_V4Seq_806R: 5' GGACT ACNNGGGTATCTAAT	Sigma	Caporaso et al.[55]
Software and algorithms		
Graphpad Prism 9.4	GraphPad Software, Inc.	N/A
R Studio 2022.07.01	R Studio	https://cran.r-project.org/
Quantitative Insights into Microbial Ecology (QIIME) v1.8.0	Caporaso et al.[55]	N/A
FastTree	Price et al.[56]	N/A
Ribosomal Database Project (RDP) classifier	Wang et al.[57]	N/A
OTU picking with UCLUST	Edgar[58]	N/A
PyNAST alignment	Price et al.[56]	N/A
Phyloseq	McMurdie and Holmes[59]	N/A

RESOURCE AVAILABILITY

Lead contact

Further information should be requested from the lead contact, Prof. Dr. Till Strowig (till.strowig@helmholtz-hzi.de).

Materials availability

All strains used in this study are available from the DSMZ or the lead contact, if necessary, with a completed Materials Transfer Agreement.

Data and code availability

- 16S rRNA gene sequencing data from mice have been deposited in the NCBI (Bioproject Database) under the accession number: PRJNA809685. 16S rRNA gene sequencing data from piglets are available at the Sequence read archive (SRA) under the BioProject accession number PRJNA800240. The RNA sequencing data from the in vitro experiments are available at the Sequence read archive (SRA) under the BioProject accession number PRJNA949940. The mass spectrometry proteomics data have been deposited to the ProteomeXchange Consortium via the PRIDE partner repository with the dataset identifiers PXD029243.
- This paper does not report original code.
- Any additional information required to reanalyze the data reported in this work is available from the lead contact upon request.

EXPERIMENTAL MODEL AND STUDY PARTICIPANT DETAILS

Ethics statement

All animal experiments were performed in agreement with the guidelines of the Helmholtz-Zentrum für Infektionsforschung, Braunschweig, Germany, the national animal protection law (Tierschutzgesetz (TierSchG), the animal experiment regulations (Tierschutz- Versuchstierverordnung (TierSchVersV)), and the recommendations of the Federation of European Laboratory Animal Science Association (FELASA). The mice study was approved by the Lower Saxony State Office for Nature, Environment and Consumer Protection (LAVES), Oldenburg, Lower Saxony, Germany; permit No. 33.19-42502-04-19/3266. The pig study protocol was approved by the Thüringer Landesamt für Verbraucherschutz, Bad Langensalza, Germany (approval number 22-2684-04-BFI-17-001).

Mice

C57BL/6N SPF mice were purchased from Janvier-Labs and maintained (including housing) at the animal facilities of the Helmholtz Centre for Infection Research (HZI) under enhanced specific pathogen-free (SPF) conditions for at least two weeks before the start of the experiment. Female and male mice with an age of 6 – 30 weeks were used. Germfree C57BL/6NTac mice were bred in isolators

(Getinge) in the germfree facility at the HZI. Sterilized food and water ad libitum was provided. Mice were kept under a strict 12-hour light cycle (lights on at 7:00 am and off at 7:00 pm) and housed in groups of up to six mice per cage in airtight and individually ventilated ISOcages containing a HEPA-filter (Techniplast) to prevent cross-contamination and the spread of *C. difficile* spores according to biosafety guidelines at our institution. During mice experiments, no mice were transferred between cages and every experimental group was kept to their own cage. All mice were humanely euthanized by asphyxiation with CO_2 and cervical dislocation.

Pigs

Female piglets (*Sus scrofa domestica*) aged four weeks were obtained from the Mörsdorfer Agrar GmbH (Mörsdorf, Thuringia, Germany) and were in quarantine at the animal facility of the Friedrich-Loeffler-Institute (Jena, Germany) for two weeks before starting the experiment. Piglets received feed and water *ad libitum*. The animals were housed in groups of up to four piglets per conditioned box, enrichment and red light was provided. Health conditions were determined daily. All piglets were euthanized by the application of Release (0.9 mL/ 5 kg body weight).

Bacterial strains and growth conditions

Origins of all strains used in this study are listed in the key resources table. Strains were routinely grown in Brain Heart Infusion Broth (BHI, Oxoid) or BHIS medium (BHI 37 g/L, 5% yeast extract, 1% L-cysteine, 1 mg/l vitamin K, 5 mg/l hemin) in an DG250 anaerobic work-station (Don Whitley Scientific, Bingley, Great Britain; 98% N_2, 2% H_2) or Coy Laboratories anaerobic chamber (85% N2, 10% CO_2, and 5% H_2) at 37 °C. If appropriate, *C. difficile* minimal medium (CDMM) was used.[60] *C. difficile* spores were kept at 4 °C and were inoculated in BHI medium (Oxoid) with 0.1% taurocholic acid to allow spore germination. All other strains were kept at -70 °C and were inoculated in BHI from glycerol stocks.

METHOD DETAILS

MIC/MBC determination for chlorotonils

Fresh cultures were grown to exponential phase (OD_{600}= 0.2 – 0.5) and cell density was adjusted to $1x10^6$ CFU/mL before inoculation. Chlorotonils, fidaxomicin and metronidazole were dissolved in DMSO, vancomycin in ddH2O and diluted in a two-fold dilution series starting from 12.8 μg/mL to 25 ng/mL (6.4 μg/mL to 6.25 ng/mL for Fidaxomicin) in 100 μL BHIS media. Antibiotic containing media were then inoculated with 100 μL bacterial culture, resulting in a total volume of 200 μL BHIS with a final concentration of $5x10^5$ CFU/mL and 6.4 μg/mL to 12.5 ng/mL (3.2 μg/mL to 3.125 ng/mL for Fidaxomicin) antibiotic concentration per well. For MBC determination, 50 μL of each well without visible growth (and with growth as controls) were plated on BHIS agar and further incubated for 24h at 37°C. OD_{600} values for growth curves were acquired using a LogPhase 600 4-plate reader for 24h (BioTek) and blanked against BHIS. OD_{600} values below 0.005 were adjusted to 0.005 and set as detection limit. All MIC/MBC values were determined in three independent biological replicates with four technical replicates each.

Bacterial spore preparation & purification

Bacterial spores were generated as previously described with minor changes.[61] Briefly, *C. difficile* was grown overnight under anaerobic conditions. Cells were harvested by centrifugation, washed twice with 1x PBS and OD_{600} was adjusted to 0.2. Cells were spread on BHIS agar (+ 0.1% TCA) and incubated at 37°C for 7 days under anaerobic conditions. Spores were harvested by adding 1 mL 1x PBS to the plate, collected using cell spreader and transferred into 2 mL reaction tubes. Spores were pelleted by centrifugation at 14,000 × g, supernatant discarded and resuspended and washed twice in 2 mL 1x PBS. To kill all remaining vegetative cells, the spores were heat-treated at 65°C for 20 minutes. Spore count was determined by 10-fold dilution series plated on BHIS agar plus 0.1% TCA. Spore purification was performed by 50% sucrose gradient centrifugation followed by 5x washing in sterile 1x PBS. Spores were stored at 4°C in glas-tubes. The purity and concentration of the *C. difficile* VPI 10463 spore-stock was not sufficient to perform the highly sensitive 'loss of OD_{600}' and persistence assays, even after repeated purification. Hence, we utilized *C. difficile* 630 spores for these experiments.

Inhibition of spore outgrowth

Purified *C. difficile* spores were treated with different concentrations of ChA, ChB1-Epo2, vancomycin, metronidazole and fidaxomicin for 1h at 37°C shaking at 800 rpm. To determine CFUs, serial dilutions of treated spores were plated on BHIS agar, supplemented with 0.1% TCA and incubated for 24 - 72 h, depending on the experiment. The two lowest dilutions with at least 10 colonies were used to determine CFUs. For *in vitro* germination in liquid media, treated spores were washed three times with 1x PBS, inoculated into BHIS + 0.1% TCA media and growth was monitored by LogPhase 600 4-plate reader for 48h (BioTek). OD_{600} values below 0.005 were adjusted to 0.005 and set as detection limit. Washing of *C. difficile* spores with different solvents was performed as follows: After antibiotic incubation, spores pellets were washed with 1 mL 1x PBS, 10% EtOH or 70% EtOH 5 times, with a transfer of spores to a new Eppendorf tube between wash 4 and 5 to prevent antibiotic carryover. Spore pellets were then washed twice with 1x PBS to prevent growth inhibition by remaining EtOH, followed by serial dilution and plating on BHIS + 0.1% TCA agar.

Loss of OD_{600} germination assay

Adapted from Hopkins and Wilson.[46] Purified *C. difficile* 630 spores were pelleted and resuspended in 50 mM Tris-HCL (pH 7.4) and OD adjusted to ≈ 0.5. Germination was determined by measuring OD_{600} every minute over a time of 60 minutes at 37°C in a BioTek

Synergy H1 microplate Reader following addition of germinants. Germination was induced by a final concentration of 0.1% TCA, 50 mM glycine and 60 mM $CaCl_2$. Results are reported as % of initial OD_{600}.

Determination of chlorotonil persistence by large plate *B. subtilis* bioassay

Adapted from Dharbhamulla et al.[44] and Mullish and Williams[45] Fresh *B. subtilis* cultures were grown aerobically in BHIS media at 37°C until late exponential phase (OD_{600} = 0.5 - 1.0). OD_{600} was adjusted to 0.5 and 1mL of culture was inoculated into 30 mL BHIS-Agar (50°C) and poured into 245 mm x 245 mm bio-assay dishes. TCA was omitted from plates, to prevent germinating *C. difficile* spores from potentially inhibiting *B. subtilis* growth. Once the plates dried, 10 μL spore solution of ChA, ChB1-Epo2 or fidaxomicin (6.4 μg/mL) treated and washed spores were inoculated on top of the *B. subtilis* agar. As control, 10 μL antibiotic solution (in DMSO) in decreasing concentrations were inoculated onto the same plate (spatially separated). Bioassay-plates were incubated aerobically for 24h and pictures of inhibition zones were taken.

Piglet feeding trial

The piglets (n = 2 per group in pre-trial, n = 4 per group in main trial) were fed two times with an interval of 24h either peanut butter or ChA (10 mg per kg body weight) mixed with peanut butter. Sample collection and handling was performed as follows: Individual stool samples were collected every 24h and immediately homogenized and split. Aliquots were stored in DNA stabilization solution (STRATEC SE, Birkenfeld, Germany) for sequencing of 16S rRNA gene amplicons. Remaining sample volume was stored at -20°C without additives.

Mice antibiotic treatment

SPF mice were weighted and fresh feces samples were taken. ChA and ChB1-Epo2 were dissolved in soy oil (Oleum Sojae raffinatum, Caesar & Loretz GmbH) at 40°C in an ultrasonic bath for 3 × 5 minutes. Chlorotonil solutions were mixed by pipetting up and down before every gavage. Chlorotonils were administered at concentration of 40 mg/kg and 20 mg/kg by oral gavage and vancomycin at a concentration of 20 mg/kg dissolved in 1x PBS in 100 – 200 μL solvent, depending on the weight of the mice.

Mice infection with *C. difficile*

All infection experiments were performed with *C. difficile* strain VPI 10463. Each experimental group was housed in separate cages prior and during infection experiments. Infected mice were monitored and scored daily for symptoms of clinically severe CDI including fur, skin, provoked behavior, weight loss, feces consistency, and posture. Mice showing signs of CDI were monitored twice a day and humanely euthanized after losing 20% of their initial weight or developing severe clinical signs of features listed above and counted as 'death' in Kaplan-Meier survival plots. Spores were heat-treated at 65°C for 20 minutes and counted by plating 24h before every infection, to determine infection dose. After different time points, mice were humanely euthanized by asphyxiation with CO_2 and cervical dislocation and samples for further analysis were extracted.

SPF mice

SPF mice were weighted and treated with 10 mg/kg clindamycin 24h prior to infection, administered via intraperitoneal injection to induce susceptibility to *C. difficile* infection.[62] For the ChA pre-treatment experiment, mice were treated with either ChA (40 mg/kg) or soy oil (control) in parallel to clindamycin treatment, administered via oral gavage. On the following day, mice were infected with 10^4 *C. difficile* spores in 200 μL 1x PBS administered via oral gavage. Spores for infection with ChA-treated spores were generated as follows: *C. difficile* VPI10463 spores were treated with 6.4 μg/mL ChA for 1 h at 37°C shaking at 800 rpm. Following incubation, spores were washed five times in 1x PBS with transfer of spores to a new Eppendorf tube between wash 4 and 5 to prevent antibiotic carry-over.

Germ free mice

Germ free C57BL/6N mice were bred in isolators (Getinge) in the germ free facility at the HZI. Due to lack of colonization resistance in GF mice, no antibiotic pre-treatment was administered before infection and mice were infected with a reduced dose of 10^3 *C. difficile* spores in 200 μL 1x PBS administered via oral gavage.

Quantification of *C. difficile* colonization

Fresh fecal samples were collected at different infection time points, and weight was recorded. Subsequently, fecal samples were diluted with 5 mL 1x PBS and homogenized 30 seconds at 30,000 rpm using a Polytron PT 2500E dispersing device. *C. difficile* quantification in Figure 7 was performed with an improved protocol and additionally from fecal samples from d1 p.i., leading to a lower detection limit for this experiment, compared to experiments in Figures 3D and 6F. Briefly, fecal samples were diluted in 1mL 1x PBS, including approximately 100 mg 0.1 mm zirconia beads, and homogenized using Mini-BeadBeater-96 for 50 seconds. To determine CFUs, serial dilutions of homogenized samples were plated on bioMérieux™ *C. difficile* agar. For the quantification of spores, vegetative cells were heat killed at 65°C for 20 min and plated on *C. difficile* agar pre-treated with 0.1% TCA to induce germination. Plates were cultured at 37C for 48h in anaerobic boxes before counting. CFUs of *C. difficile* were calculated after normalization to the feces weight.

Lipocalin-2/*C. difficile* toxin ELISA

Fecal samples from mice were weighed and stored at -80°C prior to ELISA measurement. Fecal samples were transferred into 2 mL screw top reaction tubes containing roughly 100 mg of 0.1 mm zirconia/silica beads (Roth), mixed with 500 μL Dilution Buffer and put on ice for 30 min. Subsequently samples were homogenized using a Mini-BeadBeater-96 (BioSpec) for 10 seconds and centrifuged for 5 minutes at 2500 × g to remove any particle matter. Supernatant was used for determination of fecal Lipocalin-2 or *C. difficile* toxin levels using the following ELISA kits "Mouse lipocalin-2/NGAL DuoSet ELISA (DY1857)" (R&D Systems) and "Separate detection of *C. difficile* toxins A and B (TGC-E002-1)" (tgcBIOMICS). ELISA kits were followed to the manufacturer's instructions with the following changes: Lipocalin-2 assay was scaled down to fit 96-well costar assay plates (CORNING).

Bile acid extraction from mice feces

Fecal samples were mixed with methanol (20 μL per mg sample) and cell disruption was achieved in a bead beater with two cycles of 20 seconds. Samples were centrifuged for 5 min at 17,000 × g and 50% of the added methanol volume was transferred to a new reaction tube. The remaining biomass was again mixed with methanol (20 μL per mg sample) and extracted a second time by bead beating (2 cycles of 20 seconds). After centrifugation (5 min at 17,000 × g) 100% of the added methanol volume was taken and combined with the first extract. 350 μL of the combined extracts were evaporated to dryness using a vacuum concentrator and dried extracts were stored at -20 °C until further processing.

Bile acid analysis by HPLC-MS/MS

Dried extracts were resolved in 35 μL methanol (LC-MS grade) and filtered through a cellulose acetate spin filter by centrifugation at 17,000 × g for 2 min. 20 μL of the filtered extract was mixed with 4 μL of internal standard mix solution (GCDCA-d4 and LCA-d4, 0.5 mM each) and transferred to a plastic vial for HPLC analysis. BA were analyzed on an Agilent 1290 Infinity II LC-System coupled to an Agilent 6545 Quadrupol-time-of-flight mass spectrometer (Agilent Technologies) equipped with an electrospray ionization interface. One μL sample was injected and separation was performed on a Supelco Ascentis Express C18 column (75 × 2.1 mm, particle size 2.7 μm) at 22 °C with a constant flow of 300 μL/min. The following gradient was applied, using the solvents A: 5 mM ammonium formiate, pH 4 and B: methanol:acetonitrile (3:1 v/v): 0 min 55% B 2 min 68% B, 5 min 69% B, 9.50 min 85% B, 10.5 min 85% B, 12 min 100% B, 14 min 100% B, 15 min 55%, 18 min 55% B. MS analysis was done in negative ion mode with a capillary voltage of 4,000 V. Mass spectra were recorded in the range of 300-1000 m/z. Raw data was processed with the Mass-Hunter Qualitative Navigator Software (version B.08.00, Agilent Technologies) and identification of BA was achieved by using the accurate mass of the [M-H]- and/or the [M+FA-H]- ions as well as the retention times of commercially available BA standards. Data was normalized to the peak areas of the deuterated internal standards, where GCDCA was used for conjugated BA and LCA for non-conjugated BA. For quantification a 14-point calibration curve for each BA was used covering a concentration range of 0-1000 mM.

Detection of short-chain fatty acids from murine feces

The extraction and GC method was adapted from Su et al.[55] and modified in Neumann-Schaal et al.[60] Briefly, samples were resuspended in water spiked with o-cresol as internal standard (30 μl/mg sample) and homogenized. 400 μl of the mixture was acidified with 50 μl H2SO4 (HPLC grade), vigourously mixed and extracted with 200 μl *tert*-methylbutylether. The ether phase was analysed using an Agilent GC-MSD system (7890B coupled to a 5977 GC) equipped with a high-efficiency source (HES), a quadrupol mass spectrometer and a Gerstel RTC system. Chromatography was carried with an Agilent VF-WAX-ms column (30 m length, 0.25 mm inner diameter, Agilent, Santa Clara, CA, USA) applying a constant flow of 1 mL/min helium. The temperature program was as follows: 55 °C for 1 min, temperature ramping of 10 °C min to 250 °C constant for 2 min. Solvent delay time was 2.4 min. A retention index marker (n-alcanes ranging from C10…C22 in cyclohexane) was used to convert retention times to retention indices. Quantification was performed using an external calibration curve with authentic standards. Data analysis was performed as previously described.[60,58]

Detection of non-volatile metabolites from mice feces

Non-volatile organic acids and amino acids were analyzed as described in Will et al.[63] Briefly, samples were resuspended in water (20 μl per mg wet weight), homogenized in an ultrasonic bath for 10 min at room temperature and 20 μl of the sample were spiked with 100 μl methanol containing ribitol as internal standard. After centrifugation, the cleared supernatant was dried in a vacuum concentrator for 1 h. Analysis was performed on an Agilent GC-MSD system (7890B coupled to a 5977 GC) equipped with a high-efficiency source (HES), a quadrupol mass spectrometer and a Gerstel RTC system. A two-step derivatization with a methoxyamine hydrochloride solution (20 mg ml−1 in pyridine) and N-methyl-N-(trimethylsilyl)-trifluoracetamide was automatically performed with the RTC system. One microliter of the sample was injected using a multimode inlet in pulsed splitless mode (30 psi until 0.75 min, 50 ml min−1 at 1 min) and in pulsed split mode with a split ratio of 10:1 (split flow of 12 ml min−1). Separation was conducted on an Agilent VF-5ms column with a helium flow of 1.2 ml min−1. The oven temperature was held at 70 °C for 6 min and then linearly increased with 6 °C min−1 up to 325 °C. Ions were detected in scan mode from 70 to 700 m/z with 2.3 scans s−1. Quantification was performed using an external calibration curve with authentic standards. Data analysis was performed as previously described.[60,58]

Extraction and measurement of chlorotonil A and vancomycin from feces

All feces samples were lyophilized prior to extraction. For chlorotonil extraction, feces were resuspended in a respective amount of Milli-Q water (1 mL per 35 mg of dry feces) followed by the addition of an equal amount dichloromethane (DCM, HPLC grade). For

homogenization, samples were vortexed (2x10 seconds) and placed in an ultrasonic bath for at least 5 minutes. Subsequently, samples were left on a rotary shaker for 1 h (180 rpm) and were then centrifuged (100 rpm, 5 min) to aid phase separation. The lower (organic) phase was collected using glass pipettes and the DCM extraction was repeated. Samples were dried under steady nitrogen flow, resuspended in 150 μL isopropanol (HPLC grade) and prepared for HPLC-MS/MS analysis. Of note, for d7 mice samples modified extraction steps were necessary due to high protein content. Here, feces were transferred to a separation funnel and extracted using higher volumes of Milli-Q water and DCM (5 mL per 35 mg feces). The lower phase containing chlorotonils and lots of precipitate was then transferred to an additional separation funnel containing heptane and saturated saline solution. Heptane/DCM/chlorotonil formed the upper phase (density shift), while the precipitate remained in the lower aqueous phase allowing for proper separation. The organic phase was collected and dried in a rotary evaporator. The extract was resuspended in DCM and transferred to a fresh glass vial prior to nitrogen evaporation and preparation for HPLC-MS analysis. Vancomycin extraction was adapted from Hu et al.[57] Briefly, dried feces were extracted using 10% acetonitrile in Milli-Q (v/v) (1 mL per 35 mg). Samples were vortexed for 10 s and placed in an ultrasonic bath for 30 minutes and again vortexed for 10 s. Subsequently, supernatant was collected after centrifugation (15000 rpm, 10 min, 4 °C) and stored at -80 °c until further analysis. For calibration standards (n=2), feces of untreated mice were extracted and then spiked with different concentrations of ChA or Vancomycin to avoid any matrix effects. Samples of untreated animals served as extraction blanks. Feces samples were analyzed with a Vanquish UHPLC system coupled to a TSQ Altis Plus (Thermo Fisher, Dreieich, Germany) using a Hypersil Gold C18 column (1.9 μm, 50x2.1 mm, Thermo Fisher, Dreieich, Germany) and eluent A water + 0.1% formic acid, eluent B acetonitrile + 0.1% formic acid. HPLC and MS conditions were as follows: Vancomycin: HPLC: 0 – 0.25 min 90% A, 0.25 – 0.6 min 90% A – 10% A, 0.6 – 1.5 min 10% A, 1.5 – 2.0 min 90% A; MS: SRM, positive mode, Spray Voltage 3791 V, Sheath gas pressure 35 psi, Auxiliary gas pressure 30 psi, Sweep gas pressure 2 psi, Ion Transfer Tube 380°C, Vaporizer Temperature 325°C, Q1 mass 725.25 Da, Q3 mass 1307 Da, Collision Energy 14.8 V, RF lens 71 V. LOD <0.001 ng/ml. Chlorotonil A: HPLC: 0 – 0.7 min 90% A, 0.7 – 1.4 min 90% A – 10% A, 1.4 – 4.2 min 10% A, 4.2 – 5.0 min 90% A; MS: SRM, positive mode, Spray Voltage 1546 V, Sheath gas pressure 35 psi, Auxiliary gas pressure 30 psi, Sweep gas pressure 2 psi, Ion Transfer Tube 380°C, Vaporizer Temperature 350°C, Q1 mass 479.05 Da, Q3 mass 267.13 Da, Collision Energy 16.1 V; 295.05 Da, Collision Energy 13.9 V, RF lens 123 V. LOD: 100 ng/ml.

Analysis of fecal ChA bioactivity by bioassay with *S. aureus* indicator strain

To determine the bioactivity of ChA from piglet feces, 0.1 g of fecal samples were suspended in 10 mL NaCl, thoroughly vortexed, and filtered via a 0.5 μm membrane. The resulting suspension was sterilized with a 0.2 μm filter. An overnight culture of *S. aureus* was diluted 1:1,000 into LB medium with sterilized fecal suspension at a concentration of 10% (v/v). Aliquots were inoculated into 96-well microtiter plates and incubated in an automatic plate reader (Epoch2T; BioTek, Bad Friedrichshall, Germany) for at least 18 h at 37°C. Growth was determined by OD_{600}. For standardization, *S. aureus* was diluted into LB medium containing 10% of a filtered suspension of feces from untreated animals. The suspension was spiked with different concentrations of ChA.

16S rRNA gene amplification and sequencing of mice fecal samples

Feces samples were collected and stored at -20°C until processing. DNA was isolated with Zymo Research 96-well DNA extraction kits. Briefly, feces samples were transferred into 96-well bashing bead lysis rack, diluted with 650 μL lysis buffer and homogenized using a Mini-BeadBeater-96 for 3 times 5 minutes. Samples were kept in ice for 5 minutes between bead beating steps. Subsequently, the homogenate was centrifuged at 4000 × g for 20 min. 400 μL of supernatant was transferred into 2 mL 96 deep well plate (Nunc™) and centrifuged again for 20 min to thoroughly remove debris, particles and beads. 200 μL of the supernatant was used for DNA isolation and purification. Samples were purified using 96-well Zymo Magkit on a TECAN Fluent® Automation Workstation. 16S rRNA gene amplification of the V4 region (F515/R806) was performed according to an established protocol previously described.[56] Briefly, DNA was normalized to 25 ng/μl and used for sequencing PCR with unique 12-base Golary barcodes incorporated via specific primers (obtained from Sigma). PCR was performed using Q5 polymerase (NewEnglandBiolabs) in triplicates for each sample, using PCR conditions of initial denaturation for 30 s at 98C, followed by 25 cycles (10 s at 98C, 20 s at 55C, and 20 s at 72C). After pooling and normalization to 10 nM, PCR amplicons were sequenced on an Illumina MiSeq platform via 250 bp paired-end sequencing (PE250). Using Usearch8.1 software package[59] the resulting reads were assembled, filtered and clustered. Sequences were filtered for low quality reads and binned based on sample-specific barcodes using QIIME v1.8.0.[64] Merging was performed using -fastq_mergepairs–with fastq_maxdiffs 30. Quality filtering was conducted with fastq_filter (-fastq_maxee 1), using a minimum read length of 250 bp and a minimum number of reads per sample = 1000. Reads were clustered into 97% ID OTUs by open-reference OTU picking and representative sequences were determined by use of UPARSE algorithm.[59] Abundance filtering (OTUs cluster > 0.5%) and taxonomic classification were performed using the RDP Classifier executed at 80% bootstrap confidence cut off.[65] Sequences without matching reference dataset, were assembled as de novo using UCLUST. Phylogenetic relationships between OTUs were determined using FastTree to the PyNAST alignment.[66] Resulting OTU absolute abundance table and mapping file were used for statistical analyses and data visualization in the R statistical programming environment package phyloseq.[67]

Sequencing of 16S rRNA gene amplicons and data analysis of piglet fecal samples

Piglet feces were collected in 600 μL DNA stabilization solution (STRATEC SE) and stored at RT. The isolation of chromosomal DNA was carried out according to Lagkouvardos et al.[68] Raw reads were processed with the Integrated Microbial Next Generation Sequencing (IMNGS) pipeline[69] based on UPARSE.[59] Sequences were demultiplexed, trimmed to the first base with a quality

score < 3, and then paired. Assemblies with a size < 250 and > 650 nucleotides or an expected error > 3 were excluded. Remaining reads were trimmed by 5 nucleotides at each end to prevent the analysis of regions with distorted base composition. The presence of chimeras was tested with UCHIME.[70] Operational taxonomic units (OTUs) were clustered at 97% sequence identity, and only those with a relative abundance $\geq$ 0.5% in at least one sample were kept. Taxonomies were assigned at 80% confidence level by taking into account results from both the RDP classifier[65] and SINA (v1.2.11).[71] All further analyses were performed in the R programming environment using Rhea.[72] A PERMANOVA test (vegan::adonis) is performed in each case to determine if the separation of sample groups is significant, as a whole and in pairs. Counts are by standard normalized via simple division to their sample size and then multiplication by the size of the smaller sample, thus avoiding to introduce random variance or loss of data. β-diversity was computed based on generalized UniFrac distances.[73] α-diversity was assessed on the basis of species richness and Shannon effective diversity[74] as explained in detail in Rhea. P values were corrected for multiple comparisons according to the Benjamini-Hochberg method. Only taxa with a prevalence $\geq$ 30% (proportion of samples positive for the given taxa) in one given group were considered for statistical testing.

Preparation of samples for transcriptome, proteome and ICP analyses

C. difficile strain 630 was grown in CDMM to mid-exponential phase and stressed with a sublethal concentration of 4.6875 ng/mL ChB1-Epo2 or an equal volume of DMSO. For transcriptome analysis, cultures were grown for further 30 min, and harvested by centrifugation. Resulting cell pellets were washed once with TRIS-EDTA (TE) buffer (Roth, Karlsruhe, Germany), suspended in RNAlater™ Stabilization Solution (ThermoFisher Scientific, Waltham, Massachusetts, USA), and kept at 4 °C. For proteome analysis, cultures were grown for 90 minutes in the presence of the antibiotic and were harvested by centrifugation. Cell pellets were washed once with TE buffer and were directly stored at -70 °C. Samples for metallome analysis were prepared analogous to the proteomic samples but EDTA-free TRIS buffer was applied for washing and cell disruption.

RNA isolation from *C. difficile*

RNA was extracted and purified from 15 mL of a *C. difficile* culture using a RNeasy Kit (QIAGEN GmbH, Hilden, Germany) according to the manufacturer's instruction. Briefly, the bacterial pellet was washed in 200 µL PBS (manufacturer). The pellet was solved in 200 µL TE buffer with 3 mg/mL lysozyme and incubated for 15 min at RT. For further cell lysis, 700 µL RTL buffer and 50 mg 0,1mm zirconia beads were added, and the suspension vortexed three times for 45 seconds. The lysate was centrifuged for 2 min at 11,000 *g*, and 450 µL of ethanol were added. The RNA was bound to a column via centrifugation for 15 s at 10,000 *g*, and 350 µL of RW1 buffer was added to desalt the silica membrane, followed by centrifugation for 15 s at 10,000 *g*. 80 µL of a reaction mixture containing 10 µL DNase I and 70 µL buffer RDD (both Qiagen) were applied onto the silica membrane of the column and incubated at RT for 15 min. The membrane was washed with 350 µL of RW1 buffer (15 s at 10,000 *g*), and again incubated with DNase I reaction mixture for 15 min. After that, the membrane was successively washed with 350 µL buffer RW1 (15 s at 10,000 *g*), and with 500 µL buffer RPE (15 s at 10,000 *g* and 2 min at 11,000 *g*, respectively). Finally, the RNA was eluted in 30 µL of RNAse-free H_2O. RNA quality was assessed using a 2100 Bioanalyser (Agilent, Waldbronn, Germany).

Transcriptome analysis

Whole-transcriptome RNA library preparation with isolated RNA was performed as follows. Briefly, ribosomal RNAs were depleted using the Ribominus Transcriptome isolation Kit (Invitrogen/ Thermo Fisher Scientific), and the kit NEBNext Ultra II RNA Library Prep (New England Biolabs, Ipswich, Massachusetts, USA) was used for library construction. The libraries were diluted and sequenced on a MiSeq sequencer (Illumina, Munich, Germany) using a MiSeq Reagent Kit v2 (50 cycles), resulting in 50 bp single-end reads. Illumina FASTQ files were mapped to the reference genome of C. difficile (NC_009089) using Bowtie for Illumina implemented in Galaxy.[75] Galaxy also was used to visualize and calculate the number of reads mapping on each gene. Gene counts of each library were normalized to the smallest library in the comparison and RPKM (reads per kilobase per million mapped reads) values were calculated. Fold changes between the different conditions were calculated. Statistical analyses were performed as described for every experiment. P values $\leq$ 0.05 were considered as mentioned in the text.

Extraction of proteins

Proteins were extracted from cell pellets as described previously.[76] Briefly, cell pellets were suspended in 1 mL TE buffer and lysed by mechanical disruption with 500 µL glass beads (0.1 to 0.11 mm, Satorius Stedim Biotech, Göttingen, Germany) in a FastPrep-24™ 5G homogenizer (MP Biomedicals, Santa Ana, California, USA) in three cycles at 6.5 m/s for 30 s. Glass beads and cell debris were removed by three centrifugation steps at 20,000 x g and 4 °C. Resulting protein extracts were stored at -70 °C. Protein concentrations were determined using Roti®-Nanoquant (Roth, Karlsruhe, Germany) according to the manufacturer's instructions.

LC-MS/MS sample preparation for proteome analysis

50 µg of each respective protein sample were digested on S-trap™ micro columns (ProtiFi, Huntington, New York, USA) according to the manufacturer's instructions. Briefly, protein samples were adjusted to a final concentration of 5% SDS followed by reduction of proteins with 10 mM dithiothreitol (Sigma Aldrich, St. Louis, USA) and alkylation of proteins with 20 mM iodoacetamide. Prior to load onto the S-trap™ micro columns, samples were acidified with phosphoric acid (Roth, Karlsruhe, Germany) and were diluted with 100 mM triethylamine bicarbonate (TEAB), 90% methanol in a ratio of 1:7. Columns with trapped proteins were washed four times

with 100 mM TEAB, 90% methanol. Subsequently, trypsin (Promega, Madison, USA) was added in an enzyme-to-protein ratio of 1:50 and proteins were digested at 47 °C for 3 h. For elution of digested peptides, elution buffers 1 to 3 ((1) 50 mM TEAB, (2) 0.1% acetic acid and (3) 60% acetonitrile, 0.1% acetic acid) were added to columns and peptides were eluted by centrifugation. Eluted peptides were dried by vacuum centrifugation. For peptide purification and fractionation digested peptides were suspended in 300 μL of 0.1 trifluoroacetic acid (TFA, Sigma Aldrich, St. Louis, USA) and loaded on self-packed C_{18} columns (Reprosil Gold 300 C_{18}, 5 μm; Dr. Maisch HPLC GmbH, Ammerbruch-Entringen, Germany) as done previously.[77] C_{18} columns were washed once with MS-pure water and peptides were eluted with increasing concentrations of acetonitrile in 0.1 % trimethylamine (Carl Roth GmbH, Karlsruhe, Germany) revealing eight fractions. For LC-MS/MS measurements of *in vitro* samples, fractions 1 and 5, 2 and 6, 3 and 7 and 4 and 8 of each individual sample were pooled. Finally, acetonitrile was removed by vacuum centrifugation and samples were suspended in 0.1% acetic acid directly prior to LC-MS/MS analysis.

LC-MS/MS analysis for proteome analysis

For LC-MS/MS analysis, peptides were separated by liquid chromatography using an EASY nLC 1200 directly coupled to a Q Exactive™ HF Hybrid Quadrupole-Orbitrap™ mass spectrometer (Thermo Fisher Scientific, Waltham, Massachusetts, USA). Peptides loaded onto self-packed analytical columns with integrated emitter (100 μm × 20 cm) containing C_{18} reverse phase material (3 μm, Dr. Maisch HPLC GmbH, Ammerbruch-Entringen, Germany) and were eluted using a 85 min gradient from 5 to 50% of acetonitrile, 0.1% acetic acid at a constant flow rate of 300 nL/min. Full survey scans were performed with a resolution of 60,000 in the range of 333 – 1650 m/z. MS/MS scans were performed for the fifteen most abundant precursor ions per scan cycle excluding unassigned charge states and singly charged ions and dynamic exclusion enabled for 30 s. Internal lock mass calibration was applied (lock mass 445.12003).

LC-MS/MS data analysis of proteomic data

Database search and label-free quantification (LFQ) was done using the MaxQuant proteomics software package (version: 2.0.1.0).[78] Data were searched against a protein sequence database for *C. difficile* strain 630 obtained from NCBI, August 2021 (NC_009089; 3,560 entries). Common contaminants and reverse sequences were added by the MaxQuant software. For protein identification a maximum of two missed cleavages was assumed, oxidation of methionine was set as variable modification, carbamidomethylation of cysteine was set as fixed modification and the number of minimal required unique peptides was set to one. Unique and razor peptides were considered for label-free protein quantification with a minimum ratio count of two. The option "Match between runs" was enabled within samples from each condition. *C. difficile* proteins were included in the analysis if they were identified with at least two unique peptides in at least two out of three biological replicates. Significant changes in protein intensities were identified by statistical analysis using the R package "DEqMS"[79] and were visualized as a heatmap using the R package "pheatmap."[84]

ICP-MS analyses

To determine intracellular elemental concentrations, 20 μL cellular extract were separated on a Superose 6 Increase 3.2x300 gel-filtration column by isocratic elution with 10 mM Tris-HCl, pH 7.4 at a flow rate of 100 μL min^{-1}. The eluate was directly infused into an Agilent 7500c ICP-MS instrument, equipped with a Scott type spray chamber and a PFA μ-flow nebulizer, to monitor the intensity for several elemental isotopes over a period of 100 min. The plasma was operated at 1600 W and all other parameters were optimized daily to obtain stable signals for the elements of a tuning solution (10 ppb of: 6Li – ~8.0e4 cps, 89Y - ~1.3e5 cps, 140Ce - ~1.3e5 cps, 205Tl - ~ 9.6e4 cps), as well as stable background signals for 13C, 23Na, 39K when infusing the eluent from the gel-filtration column.

Using R scripts, the obtained chromatograms for each isotope were corrected for the natural isotope abundance as provided by the instrument manufacturer and for sensitivity drifts by a smoothed 13C baseline. In order to enable comparison between the ChB1-Epo2-treated and control samples, protein content was determined by Bradford assay (BSA as external calibrant) for each sample and the chromatograms scaled according to the injected protein amount. Peak areas above the baseline were integrated for each isotope with Fityk 1.3.1[85] and total elemental content was calculated as the summarized peak area. Statistical testing and visualization were performed using the R packages "rstatix" and "ggplot2."[86,87]

QUANTIFICATION AND STATISTICAL ANALYSIS

Statistical analysis was either performed using GraphPad Prism version 9.4.0, R studio software version 2022.07.01 or Microsoft excel 2016. Error bars and statistical tests are indicated below each figure and p values < 0.05 were considered significant and classified into different significance levels: *p<0.05, **p<0.01, ***p<0.001, ****p<0.0001